(TRIM5 proteins). HIV-1 can indeed counteract human proteins corresponding to these restriction factors. APOs exhibit cytidine deaminase activity, and introduce lethal mutations into HIV-1 genome. HIV-1 Vif is able to neutralize the antiviral activity of human APOs, but not macaque APOs [6–8]. CypA acts on incoming HIV-1 core to regulate infection positively in human cells but negatively in macaque cells [9–11], though amino acid sequences of CypA from human and macaque are identical. Macaque TRIM5α recognizes and interacts with incoming HIV-1 core, and restricts virus infection in a less-defined mechanism [9–11]. Macaque TRIM5α is polymorphic, and has sequence variation in a C-terminal B30.2/SPRY domain important for capsid (CA) binding. Sequence variation in this domain causes modulation of host susceptibility to retrovirus infection [12,13]. Macaque TRIMCyp is a fusion protein resulted from replacement of a B30.2/SPRY domain with CypA. Both CyM and RhM cells express TRIMCyp, but affinity of these proteins to HIV-1 core is different due to amino acid substitutions in Cyp domains. Thus, CyM TRIMCyp restricts HIV-1 replication, but not RhM TRIMCyp [14,15].

Identification of host restriction factors in macaque cells and their target proteins in HIV-1 has prompted us to generate macaque-tropic HIV-1 (HIV-1mt) with a minimal modification of HIV-1 genome. We successfully constructed prototype HIV-1mt, NL-DT5R, by replacing CypA binding region on a loop between helices 4 and 5 (h4/5L) in *gag*-CA and entire *vif* genes with the corresponding regions of pathogenic SIVmac239 (Fig. 1) [16]. But growth potential of NL-DT5R was inferior to that of SIVmac239 both *in vitro* and *in vivo* [16,17]. These results indicated that genetic modifications in NL-DT5R were insufficient to confer the ability on the virus to grow efficiently in macaque cells [16–18]. In an attempt to improve growth potential of NL-DT5R, we adapted NL-DT5R and its R5-tropic version NL-DT562 to a CyM derived lymphocyte cell line HSC-F, and found a number of genetic substitutions in viral genomes of adapted viruses [19]. We introduced these mutations and CA h6/7L from SIVmac239 into NL-DT5R, and the resultant clone was designated MN4-5S (Fig. 1) [19]. MN4-5S exhibited enhanced growth potential in CyM both *in vitro* and *in vivo* compared to NL-DT5R [19]. But growth ability of MN4-5S was still lower than that of SIVmac239.

In this study, to further improve replication potential of HIV-1mt, we adapted MN4-5S in macaque cells and identified an adaptive mutation in CA that enhances growth ability in the cells. *In silico* structural modeling of the adaptive mutation predicted that Q110D mutation on helix 6 in CA (CA-Q110D) would promote viral replication in macaque cells. Indeed, a proviral clone carrying CA-Q110D, designated MN4Rh-3, exhibited marked enhancement of growth potential in macaque cells relative to all the other HIV-1mt clones we have constructed (Fig. 1). CyM TRIM5α/TRIMCyp susceptibility assays revealed that MN4Rh-3 completely evades from TRIMCyp restriction but not TRIM5α restriction as observed for the other HIV-1mt clones. While CA-Q110D contributed to neither endowment of further resistance to TRIMCyp nor evasion from TRIM5α restriction, CA-Q110D did lead to enhanced single-cycle infectivity to a macaque cell line compared with the other HIV-1mt clones. Our results here indicate that CA-Q110D accelerates viral growth in macaque cells independently of TRIM5 proteins restriction.

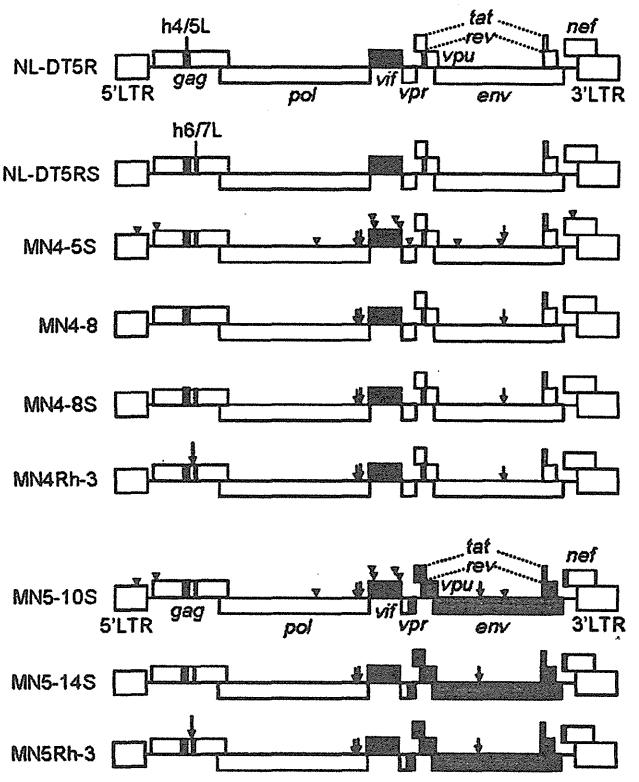

Fig. 1. Proviral genome structure of various HIV-1mt clones used in this study. HIV-1 NL4-3 [26] and SIVmac239 (GenBank: M33262) sequences are indicated by white and black areas, respectively. Gray areas in MN5-10S, MN5-14S and MN5Rh-3 show sequences from NF462 [21]. Blue arrows and black arrowheads show nucleotide substitutions that appeared in viral genomes of NL-DT5R and NL-DT562 during adaptation in HSC-F cells. Among nucleotide substitutions, adaptive mutations that enhance viral growth potential are indicated by blue arrows. Red arrows show the CA-Q110D mutation.

2. Materials and methods

2.1. Plasmid DNA

Construction of NL-DT5R, NL-DT562, NL-DT5RS, and MN4-5S were described previously [16,19–21]. MN4-5S carries all nucleotide substitutions that are present in adapted NL-DT5R and NL-DT562 clones except for mutations in the *env* gene of R5-tropic viruses (MN5-10S, MN5-14S, and MN5Rh-3 in Fig. 1) [19]. MN4-8S contains adaptive (growth-enhancing) mutations in MN4-5S but not the other mutations. MN4Rh-3 was constructed by introduction of the CA-Q110D mutation into MN4-8S. To construct R5-tropic viruses, 3′ halves of viral genomes (*Eco*RI in *vpr* to *Sph*I at the 3′ end of viral genome) of MN4-5S, MN4-8S, and MN4Rh-3 were replaced with the corresponding regions of adapted-NL-DT562,

and were designated MN5-10S, MN5-14S, and MN5Rh-3, respectively. For single-cycle infectivity assays to monitor viral susceptibility to TRIM5 proteins and to determine infectivity for CyM cells, *env*-deficient HIV-1mt variants encoding luciferase gene were constructed. NL-DT5R was cleaved with *Nde*I and *Nhe*I (both sites in *env* gene), blunt ended by T4 DNA polymerase, and resealed by T4 DNA ligase. The resultant clone was designated 5RΔEnv. Luciferase gene was then introduced into *nef* gene of 5RΔEnv as described previously [22], and the resultant clone was designated 5RΔEnv + Luc. A fragment containing the 3′ half genome was cut out from the 5RΔEnv + Luc, and introduced into the corresponding region in HIV-1mt variants (DT5R/4-3, NL-DT5RS, MN4-8, MN4-8S, and MN4Rh-3) to generate 5R/4-3ΔEnv + Luc, 5RSΔEnv + Luc, 4-8ΔEnv + Luc, 4-8SΔEnv + Luc, and 4Rh-3ΔEnv + Luc, respectively.

2.2. Cell culture

A human monolayer cell line 293T [23], a feline kidney cell line CRFK (ATCC CCL-94), and a CyM kidney cell line MK.P3(F) (JCRB 0607) were maintained in Eagles's minimal essential medium (MEM) containing 10% heat-inactivated fetal bovine serum (hiFBS). CRFK cells expressing TRIM5α/TRIMCyp were maintained in MEM containing 10% hiFBS and 400 μg/mL G418 (SIGMA). Macaque lymphocyte cell lines, HSC-F [24] and HSR5.4 [25], were maintained in RPMI-1640 medium containing 10% hiFBS. Recombinant human IL-2 (AbD Serotec) was added to the medium (50 units/mL) for maintenance of HSR5.4 cells. A human lymphocyte cell line MT4/CCR5 (MT4 cells stably expressing CCR5) was maintained in RPMI-1640 medium containing 10% hiFBS and 200 μg/mL hyglomycine (SIGMA).

2.3. Virus replication assays

Virus stocks for infection were prepared from 293T cells transfected with proviral clones as described previously [16,19,26]. Virion-associated reverse transcriptase (RT) activity was measured as described previously [16]. HSC-F cells (10^6) were infected with equal RT units of viruses in the presence of IL-2. For infection of MT4/CCR5 cells (10^6), the spinoculation method [27] was used. Viral growth was monitored by RT activity released into the culture supernatants. We assessed the viral growth potential by the peak day of virus production, and if the viral growth kinetics are similar, by the production level on the peak day.

2.4. Generation and characterization of adapted viral clones

MN4-5S and MN5-10S viruses (Fig. 1) prepared from transfected 293T cells were inoculated into HSR5.4 cells (3×10^6) with an equal amount of viruses (5×10^7 RT units). The cultures were maintained in the presence of IL-2, and HSC-F cells were added on day 34 post-infection. The culture supernatants (collected on day 18 post-cocultivation, the peak day of virus production) were inoculated into fresh HSR5.4 cells, and total DNA was extracted from the cells on day 15 post-infection. Integrated proviruses were amplified from total DNA as two overlapping fragments by the polymerase chain reaction (PCR), and amplified products were cloned into MN5-10S as described previously [16]. Viruses were prepared from 293T cells transfected with the resultant clones, and inoculated into HSR5.4 cells. Only one clone exhibited a rapid growth kinetics compared to MN5-10S, and was designated Ad clone-25. To identify an adaptive mutation that enhances growth potential, each mutation found in the genome of Ad clone-25 was introduced into MN5-14S by site-directed mutagenesis (STRATAGENE). For screening, viruses prepared from transfected 293T cells were inoculated into HSC-F cells, and virus replication was monitored by RT activity released into the culture supernatants.

2.5. Molecular modeling of HIV CA N-terminal domain (NTD)

The crystal structure of HIV-1 CA NTD at a resolution of 2.00 Å (PDB code: 1M9C [28]) was taken from the RCSB Protein Data Bank [29]. The three-dimensional (3-D) models of HIV-1 CA NTD were constructed by the homology modeling technique using 'MOE-Align' and 'MOE-Homology' in the Molecular Operating Environment (MOE) (Chemical Computing Group Inc., Quebec, Canada) as described [30–32]. We obtained 25 intermediate models per one homology modeling in MOE, and selected the 3-D models which were the intermediate models with best scores according to the generalized Born/volume integral methodology [33]. The final 3-D models were thermodynamically optimized by energy minimization using an AMBER99 force field [34] combined with the generalized Born model of aqueous solvation implemented in MOE [35]. Physically unacceptable local structures of the optimized 3-D models were further refined on the basis of evaluation by the Ramachandran plot using MOE.

2.6. Single-cycle infectivity assays

To generate CRFK cells expressing CyM TRIMCyp, the cDNA was isolated from HSC-F cells, and expression vector of FLAG-tagged CyM TRIMCyp was constructed as described previously [18]. The sequence of TRIMCyp from HSC-F cells was identical with Mafa TRIMCyp2 (GenBank: FJ609415). CRFK cell lines expressing CyM TRIMCyp were selected by G418 as described previously [18]. Expression and inhibitory effect of the selected cell clones were verified by Western blotting with anti-FLAG antibody (SIGMA) and by infection with vesicular stomatitis virus G protein (VSV-G) pseudotyped 5R/4-3ΔEnv + Luc, respectively. Assays using naïve CRFK, CRFK expressing CyM TRIM5α [18] or CyM TRIMCyp, and MK.P3(F) cells were similarly performed as described previously [36]. VSV-G pseudotyped virus stocks were prepared from 293T cells transfected with individual HIV-1mtΔEnv + Luc clones and pCMV-G (GenBank: AJ318514)

at a molar ratio of 1:1. Naïve CRFK, CRFK expressing TRIM5α/TRIMCyp and MK.P3(F) cells were infected with an equal titer of viruses (to generate approximately 10^7 relative luminescence (RLU) for naïve CRFK cells), and on day 2 post-infection, cells were analyzed for luciferase activity. Assays using recombinant Sendai virus (SeV)-CyM TRIM5α/TRIMCyp expression system were performed as described previously [31].

3. Results

3.1. An adaptive mutation G114E on helix 6 in CA (CA-G114E) enhances viral growth potential in macaque cells

An HIV-1mt variant MN4-5S replicated more slowly than SIVmac239 in macaque cells. In order to improve its growth potential, we carried out virus adaptation in a macaque lymphocyte cell line HSR5.4. Virus adaptation was performed by long-term culture of HSR5.4 cells infected with MN4-5S (X4-tropic) or its R5-tropic version MN5-10S (Fig. 1). Construction of proviral clones from adapted viruses was described in Materials and methods. We obtained only one clone (Ad clone-25) with enhanced growth potential from 100 proviral clones constructed and tested. We sequenced the entire genome of Ad clone-25, and found three non-synonymous mutations in CA (S33N, G114E, and T147A in Fig. 2A) and one synonymous mutation in integrase (IN)(a4943c in Fig. 2A). To identify an adaptive mutation that enhances growth potential, each mutation found in Ad clone-25 was introduced into a parental clone MN5-14S (Fig. 1). MN5-14S carries only growth-promoting mutations in MN5-10S, and the two clones exhibit similar growth potential in macaque cells. Viruses were prepared from 293T cells transfected with MN5-14S, Ad clone-25, or clones carrying individual mutations, and inoculated into HSC-F cells (Fig. 2A). Only one clone carrying CA-G114E exhibited similar growth kinetics to that of Ad clone-25 but not the others. This result indicates that CA-G114E is an adaptive mutation enhancing growth potential of HIV-1mt in macaque cells. This mutation is exactly the same as the previously found adaptive mutation, which enhanced growth of NL-4/5S6/7SvifS virus in human CEM-SS cells [37]. NL-4/5S6/7SvifS virus is a prototype HIV-1mt bearing the same CA with that of MN4-5S.

3.2. Molecular modeling of the CA NTD of HIV-1mt variants suggests that CA-G114E and CA-Q110D mutations have a similar positive effect on viral replication

The amino acid at position 114 is located in CA NTD. To obtain structural insights into impacts of the G114E substitution in order to improve growth capability of HIV-1mt variants in macaque cells, we conducted computer-assisted structural study: we constructed 3-D models of CA NTD of three HIV-1mt variants, CA-G114E, CA-G114Q, and MN4-5S, using homology-modeling technique (see Materials and methods). Main chain folds of the three models were indistinguishable, suggesting that 3-D position and type of side chain are critical

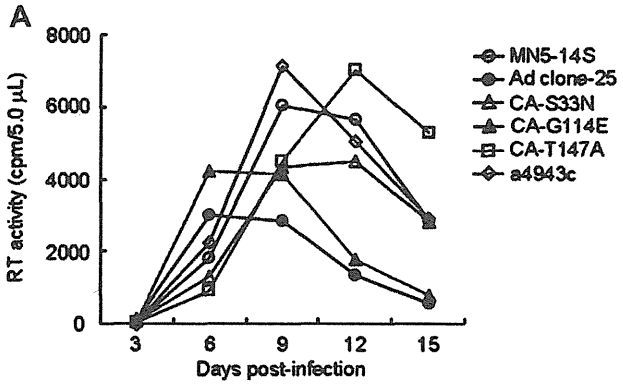

Nucleotide change	Region	Amino acid change in the region
g1283a	CA	S33N
g1526a	CA	G114E
a1624g	CA	T147A
a4943c	IN	None

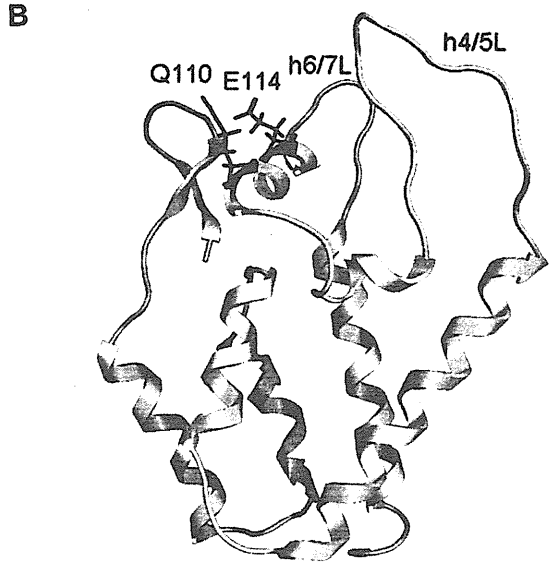

Fig. 2. Mutations in Gag-CA. (A) Identification of an adaptive mutation that enhances viral growth. Nucleotide substitutions found in the genome of Ad clone-25 are indicated at the bottom. Virus samples were prepared from 293T cells transfected with the indicated proviral clones, and equal RT units were inoculated into HSC-F cells. MN5-14S and Ad clone-25 served as controls. Virus replication was monitored by RT activity released into the culture supernatants. (B) 3-D structural models for CA NTD of HIV-1mt variants. Structural models of CA NTD of HIV-1mt variants were constructed by homology-modeling using "MOE-Align" and "MOE-Homology" in MOE as described previously [30–32]. Crystal structure of HIV-1 CA NTD at a resolution of 2.00 Å (PDB code: 1M9C [28]) was used as template for homology modeling. Main chain folds were indistinguishable among the models, and only the model of G114E CA is shown as a representative. Magenta and red sticks: side chains of 110th and 114th amino acid residues, respectively, of the G114E CA NTD.

for the phenotypic change. The modeling study revealed that 114th residue of G114E CA NTD is located on helix 6 in CA NTD such that its side chain protrudes into the exposed surface of CA (Fig. 2B). A charged amino acid residue on a protein surface participates in determining physicochemical properties of interaction surface of the protein and thus influences its structural and functional properties. Therefore, we assumed that the protrusion of a negatively charged side chain from helix 6 into exposed surface could have somehow a positive effect on growth capability of the HIV-1mt variants in macaque cells. In this regard, especially worth noting is that 110th amino acid residue on helix 6 of the HIV-1mt variant CAs was positioned on the same helical face with 114th amino acid residue (Fig. 2B). Therefore, we predicted that substitution of glutamine (Q) at position 110 by acidic amino acid such as aspartic acid (D) and glutamic acid (E) may also have a positive effect on growth capability of the HIV-1mt variants in macaque cells as G114E does. SIVmac239 has aspartic acid and glutamine at the positions 110 and 114, respectively.

3.3. CA-Q110D promotes viral growth more efficiently in macaque cells than CA-G114E mutation but its enhancing effect is species-specific

To confirm our prediction described above, CA-Q110D mutation was introduced into MN5-14S (designated MN5Rh-3), and the growth property in HSC-F cells of MN5Rh-3 and a viral clone carrying G114E (CA-G114E in Fig. 2A) was compared. As shown in Fig. 3A, MN5Rh-3 grew better than CA-G114E, indicating that CA-Q110D further accelerates HIV-1mt replication in macaque cells compared with an adaptive CA-G114E mutation. We next constructed an X4-tropic proviral clone carrying the CA-Q110D (designated MN4Rh-3) (Fig. 1), and compared its growth property with MN5Rh-3 in HSC-F cells (Fig. 3B). MN4Rh-3 was found to exhibit higher growth ability than MN5Rh-3, and was therefore used for infection experiments hereafter.

While CypA and TRIM5α have inhibitory effect on HIV-1 replication in macaque cells, CypA promotes HIV-1 infection in human cells and human TRIM5α only weakly inhibits HIV-1 replication [38–40]. Since the CA-Q110D mutation (acquisition of negatively charged side chain), as predicted by structural modeling, could impact on the interaction of HIV-1 CA and its binding factor(s) by altering physicochemical properties of CA binding surface, it can be speculated that CA-Q110D may promote viral replication specifically in macaque cells. Thus, we analyzed the effect of CA-Q110D on viral growth in macaque and human cells. In this experiment, we used HIV-1mt variants (MN4-8, MN4-8S, and MN4Rh-3) that have distinct CA structures (Fig. 1). Viruses prepared from transfected 293T cells were inoculated into macaque HSC-F and human MT4/CCR5 cells, and examined for growth property (Fig. 3C). The introduction of SIVmac239 CA h6/7L (MN4-8S) resulted in enhanced and reduced viral growth in macaque and human cells, respectively, relative to MN4-8. MN4Rh-3 grew clearly better in macaque cells relative to MN4-8 and MN4-8S, but more poorly in human cells than the other twos. These results demonstrate that the CA-Q110D mutation enhances viral replication in a host cell species-specific manner.

3.4. CA-Q110D does not contribute to evasion from CyM TRIM5 proteins restriction

We predicted that the growth enhancement by CA-Q110D may come from the increased resistance to CyM TRIM5 proteins, and therefore examined the susceptibility of HIV-1mt variants to them by two independent assays.

First, assays were performed in feline kidney CRFK cells expressing TRIM5α or TRIMCyp by using VSV-G pseudotyped viruses encoding the luciferase gene (Fig. 4A–C). The sequence differences between HIV-1mt variants reside only in CA and IN (Figs. 1 and 4). Since adaptive mutations in IN contribute to enhancement of virion production but not early replication phase (manuscript in preparation), only the difference in CA affects the relative single cycle infectivity in this assay. A pseudotyped virus 5R/4-3 carries HIV-1 (NL4-3) CA without any modifications and served as negative control. While 5R and 4-8 have an identical CA structure carrying h4/5L from SIVmac239, 5RS and 4-8S have both h4/5L and h6/7L from SIVmac239 CA. 4Rh-3 carries CA-Q110D mutation in addition to h4/5L and h6/7L from SIVmac239 CA. Viral infectivity was measured by luciferase activity in infected cells and presented as RLU. Naïve CRFK and CRFK cells expressing TRIM5α were infected with an equal amount of viruses generating 10^7 RLU in naïve cells. As shown in Fig. 4B, the infectivity of 5R and 4-8 for cells expressing CyM TRIM5α was similar to that of a negative control 5R/4-3. However, higher infectivity was observed for 5RS and 4-8S relative to 5R and 4-8. These results were consistent with previous reports that h4/5L and h6/7L in HIV-1 CA are a part of determinant for TRIM5α restriction [20,36]. The sensitivity of 4Rh-3 to TRIM5α was similar to that of 5RS and 4-8S. This indicates that CA-Q110D did not contribute to increase the resistance to TRIM5α. It has been reported that CyM TRIMCyp has the ability to restrict HIV-1 replication [15]. To examine the susceptibility of HIV-1mt variants to TRIMCyp, we generated feline CRFK cells expressing TRIMCyp, and the cells were infected with pseudotyped viruses as described above. As shown in Fig. 4C, all the clones tested were more resistant to a similar extent to TRIMCyp than the control 5R/4-3. In agreement with a previous study showing that elimination of alanine at position 88 within h4/5L of HIV-1 CA confers the resistance on the virus to TRIMCyp [15], our results indicate that the replacement of HIV-1 CA h4/5L with that of SIVmac239 is sufficient for HIV-1mt to evade from the TRIMCyp restriction. Second, we performed another susceptibility assay using the recombinant SeV expression system. This system assures a very high expression level of target proteins in cells infected with the recombinant SeV. Therefore, the ability of viruses to completely counteract the restriction effect of TRIM5 proteins could be determined by MT4/SeV-TRIM5 expression system. Human MT4 cells were infected with recombinant SeV expressing CyM TRIM5α, TRIMCyp, or SPRY(−)TRIM5, and then super-infected with HIV-1

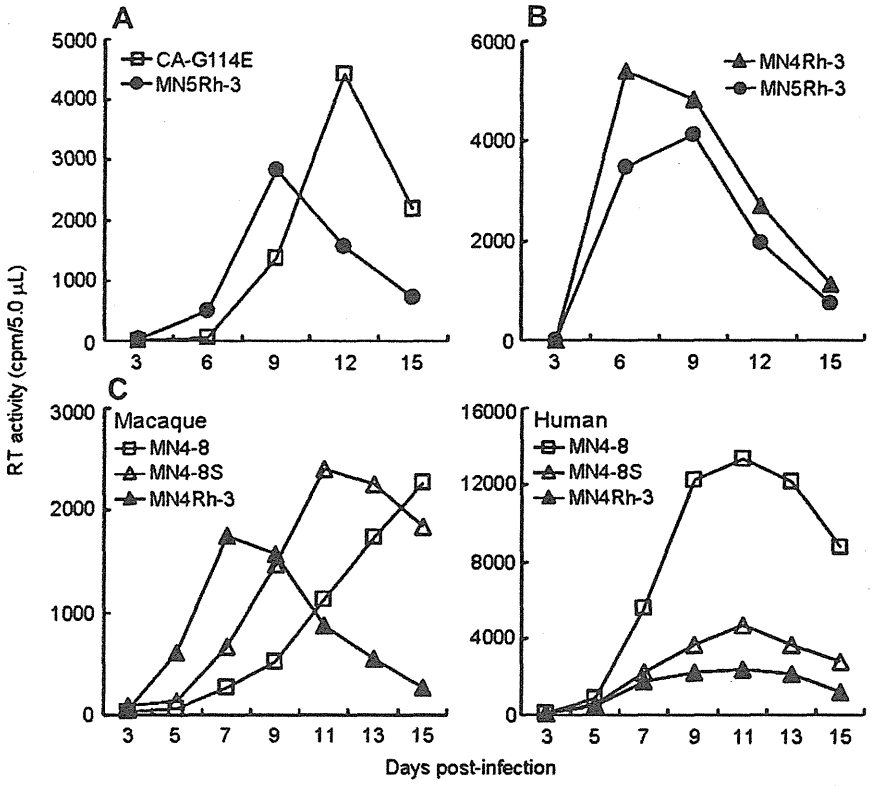

Fig. 3. Effect of CA modification on viral growth in macaque and human lymphocyte cell lines. (A and B) Growth kinetics of HIV-1mt clones carrying CA-G114E or CA-Q110D (MN5Rh-3 and MN4Rh-3) in CyM HSC-F cells. Virus samples were prepared from 293T cells transfected with the indicated proviral clones, and equal amounts (5×10^5 RT units) were inoculated into HSC-F cells (10^6). Virus replication was monitored by RT activity released into the culture supernatants. (C) Growth kinetics of MN4-8, MN4-8S, and MN4Rh-3 in HSC-F (Macaque) and MT4/CCR5 (Human) cells. Virus samples were prepared from 293T cells transfected with the indicated proviral clones, and equal amounts (10^6 RT units) were inoculated into HSC-F cells (10^6). For spinoculation of MT4/CCR5 cells (10^6), 6×10^5 RT units were used as inocula. Virus replication was monitored by RT activity released into the culture supernatants.

(NL4-3), SIVmac239, or HIV-1mt variants. SPRY(−)TRIM5 which can not bind to viral CA served as control. NL4-3 and SIVmac239 also served as controls for viral replication. As shown in Fig. 4D, NL4-3 replicated in cells expressing SPRY(−)TRIM5, but not in TRIM5α and TRIMCyp expressing cells. SIVmac239 exhibited similar growth kinetics in SPRY(−)TRIM5, TRIM5α and TRIMCyp expressing cells. All HIV-1mt variants replicated in TRIMCyp expressing cells similarly well in SPRY(−)TRIM5 cells. Together with assays in CRFK cells, these results showed that all HIV-1mt variants except for 5R/4-3 completely evade from TRIMCyp restriction. In contrast, the growth of all HIV-1mt variants was inhibited in CyM TRIM5α expressing MT4 cells. These results indicate that HIV-1mt variants do not evade from TRIM5α restriction as effectively as SIVmac239.

Results obtained by our two assay systems with respect to the susceptibility of HIV-1mt variants to CyM TRIM5α were apparently different (Fig. 4B and D), but this difference is most likely to be due to the TRIM5α expression level. In MT4 cells infected with recombinant SeV, TRIM5α is expressed at much higher level than that in transduced CRFK cells, masking the increase of resistance to TRIM5α detectable by the transduced CRFK system (Fig. 4B). Indeed, the growth enhancement of 5RS relative to 5R [20] can be explained by the results in Fig. 4B but not those in Fig. 4D. The apparent discrepancy of the sensitivity depending on TRIM5α expression level was also observed between B-LCL cells and transduced CRFK cells [41]. In sum, we can conclude here that MN4Rh-3 exhibits a partial resistance to TRIM5α insufficient for complete evasion as 5RS and 4-8S do, and that the CA-Q110D mutation is irrelevant to this property.

3.5. CA-Q110D enhances viral infectivity for macaque cells

Results so far showed that CA-Q110D does not contribute to evasion from TRIM5 proteins restriction in rather artificial systems using feline and human cells (Fig. 4). To investigate further how CA-Q110D enhances viral replication, we examined single-cycle viral infectivity in macaque cells. CyM kidney MK.P3(F) cells, which have heterozygote for TRIM5α and TRIMCyp, were infected with various VSV-G pseudoviruses and analyzed for their infectivity as described above. As shown in Fig. 5A, viral infectivity was increased by modification of h4/5L (compare 5R/4-3 and 5R&4-8). Modification of h6/7L in addition to h4/5L further augmented viral infectivity (compare 5R&4-8 and 5RS&4-8S). Introduction of the CA-Q110D mutation into 4-8S clone gave the highest infectivity among the viruses tested (see 4Rh-3). The results in

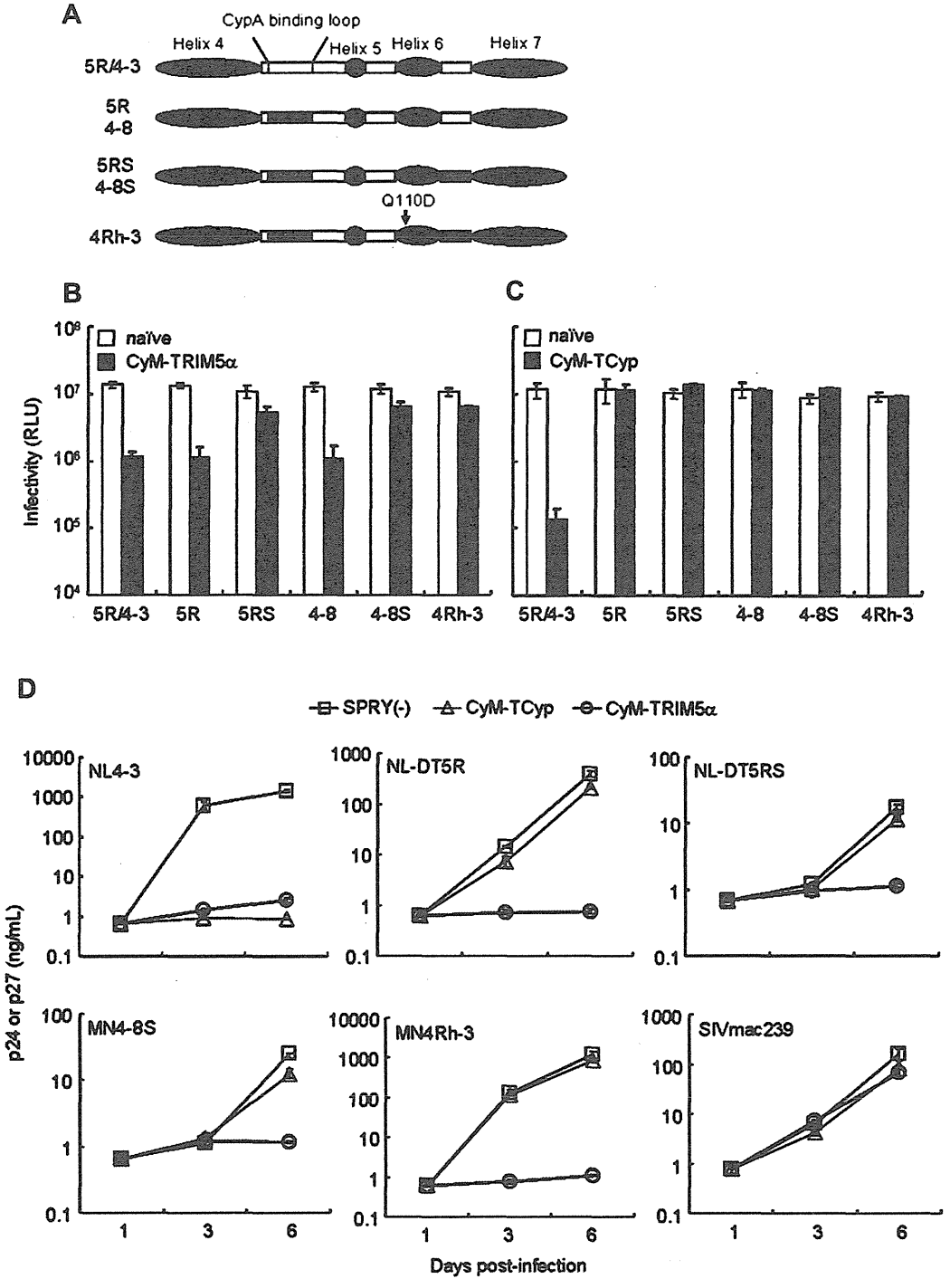

Fig. 4. Effect of CA modification in HIV-1mt variants on viral infectivity. (A) CA structure of viral clones used in TRIM5α/TRIMCyp susceptibility assays. Blue and white areas show helices and loops from HIV-1 NL4-3 CA, respectively. Sequences from SIVmac239 are indicated by black areas. (B and C) Susceptibility of HIV-1mt variants to CyM TRIM5 proteins as examined by CRFK system. Results for CyM TRIM5α (B) and for CyM TRIMCyp (TCyp) (C) are shown. VSV-G pseudotyped viruses were prepared from transfected 293T cells as input samples. Viruses generating 10^7 RLU in CRFK-naïve cells were inoculated into CRFK cells that express CyM TRIM5α or CyM TCyp. On day 2 post-infection, cells were analyzed for luciferase activity by a luminometer. (D) Susceptibility of HIV-1mt variants to CyM TRIM5 proteins as examined by SeV system. Human MT4 cells (10^5) were infected with recombinant SeV expressing CyM TRIM5α, TRIMCyp, or SPRY (−) TRIM5. Nine hours after infection, cells were super-infected with 20 ng (Gag-p24) of HIV-1 NL4-3, various HIV-1mt clones, or 20 ng (Gag-p27) of SIVmac239. Virus replication was monitored by the amount of Gag-p24 from NL4-3 and HIV-1mt clones or Gag-p27 from SIVmac239 in the culture supernatants. Error bars show actual fluctuations between duplicate samples. Data from one representative of three independent experiments are shown.

Fig. 5A show that CA-Q110D uniquely increases viral infectivity in macaque cells not observed in the other experimental systems (Fig. 4), and suggest that some factor(s) in CyM cells other than TRIM5α and TRIMCyp proteins is associated with this enhancement.

As shown in Fig. 5B, MN4Rh-3 displayed slower growth kinetics relative to those of SIVmac239 (note the peak day of virus production), although it grew better than the other HIV-1mt clones in CyM HSC-F cells. Approximately 100-fold more input virus (RT units) compared to SIVmac239 was required for MN4Rh-3 to exhibit similar growth kinetics with SIVmac239 (data not shown). These results have shown that even MN4Rh-3 grows more poorly in macaque cells than a standard SIVmac clone pathogenic for macaque monkeys.

4. Discussion

In this study, we have demonstrated that a single CA mutation (Q110D) greatly promotes HIV-1mt growth in macaque cells (Fig. 3). This enhancing effect was afforded independently of TRIM5 proteins restriction. The virus carrying the CA-Q110D mutation (MN4Rh-3) certainly overcame the anti-viral action of CyM TRIMCyp but not completely CyM TRIM5α. However, the mutation itself (Fig. 1) did not influence anti-TRIMCyp/TRIM5α activity of MN4Rh-3 reported here (Fig. 4). Notably, this mutation exquisitely enhanced viral growth in macaque cells (Fig. 3) by augmenting viral single-cycle infectivity (Fig. 5). The viral growth enhancement reported here is well reproduced in CyM peripheral blood mononuclear cells and in CyMs (manuscript in preparation).

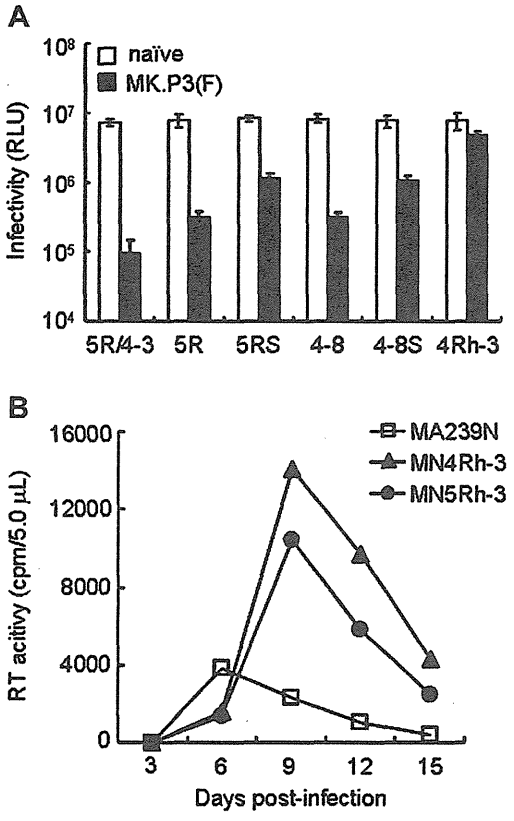

Fig. 5. Replication ability of various viruses in CyM cells. (A) Single-cycle infectivity of various HIV-1mt clones in CyM kidney MK.P3(F) cells. VSV-G pseudotyped viruses indicated were prepared from transfected 293T cells. MK.P3(F) cells were infected with an equal titer of viruses giving 10^7 RLU in CRFK-naïve cells. On day 2 post-infection, cells were analyzed for luciferase activity by a luminometer. (B) Multi-cycle growth kinetics of SIVmac and HIV-1mt viruses in CyM lymphocyte HSC-F cells. Virus samples were prepared from 293T cells transfected with the indicated proviral clones, and equal amounts (10^4 RT units) were inoculated into HSC-F cells (10^6). Virus replication was monitored by RT activity released into the culture supernatants. MA239N, an infectious clone of SIVmac239 with *nef*-open.

Regarding the mechanism for enhancement of viral growth by CA-Q110D, we initially thought a possibility that CA-Q110D compensates the disadvantage in HIV-1mt genome resulted from replacement of HIV-1 CA h4/5L and h6/7L with those of SIVmac239. However, this is highly unlikely because the enhancing effect is macaque cell-dependent (Fig. 3). Most feasible explanation is that CA-Q110D contributes to evade from a negative factor(s) in macaque cells such as CypA. Because HIV-1mt CA was designed not to bind to CypA, and the interaction between the two molecules was indeed undetectable by monitoring CypA virion-incorporation [18,20], we analyzed the binding by computer-assisted structural modeling. Homology modeling of the CA-CypA complexes was performed based on the crystal structure of HIV-1 CA NTD bound to CypA (PDB code: 1M9C [28]), and the binding energies, E_{bind}, were calculated using MOE as described previously [42,43]. As shown in Fig. 6, HIV-1 (NL4-3) CA was predicted to interact with CypA via its h4/5L (binding energy: −64.4 kcal/mol). The binding energy of CA and CypA was decreased by CA modifications, such as h4/5L replacement (NL-DT5R: −31.0 kcal/mol), h4/5L and h6/7L replacement (NL-DT5RS: −36.1 kcal/mol), and Q110D substitution in addition to h4/5L and h6/7L replacement (MN4Rh-3: −30.1 kcal/mol). Decrease in E_{bind} in NL-DT5R is consistent with the result that the h4/5L region directly interacts with CypA [28]. Notably, the E_{bind} for the NL-DT5RS CA was greater than that of the NL-DT5R and MN4Rh-3 CAs. These results suggest that not only h6/7L replacement but also Q110D substitution can influence structure of CypA binding surface of CA. The Q110D substitution is located on the exposed surface of helix 6 connecting to the h6/7L (Fig. 2B). CA helix 6 has been reported to interact with CypA binding region on h4/5L through hydrogen bonding [44,45]. Thereby it is reasonable that the local electrostatic change on the helix 6 by the Q110D substitution influenced structures of h4/5L via changes in fluctuation and conformation of h6/7L. This in turn could lead to reduction in stability of the MN4Rh-3 CA-CypA complex compared with NL-DT5RS CA-CypA complex, as predicted in Fig. 6. Our computer-assisted structural study suggests that the Q110D substitution can induce electrostatic modulation of the overall CA surface structure including h4/5L and h6/7L. Similar modulation mechanism of binding surface structures via charged amino acid substitution at distant site from the binding surface has been reported for Cyp domain of CyM TRIMCyp [15] and CD4 binding site of HIV-1 gp120 outer

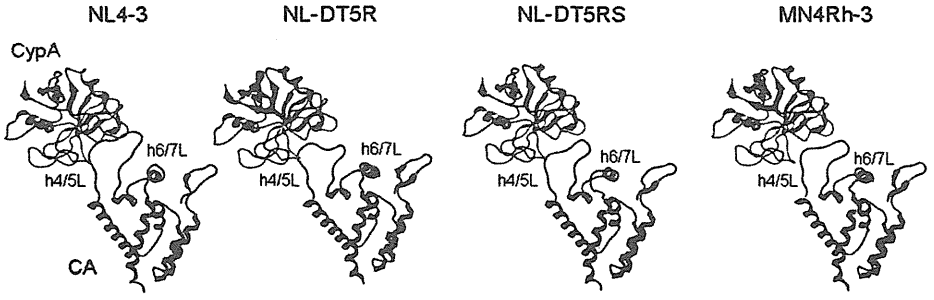

	NL4-3	NL-DT5R	NL-DT5RS	MN4Rh-3
CA	HIV-1 CA	h4/5L from SIVmac239	h4/5L and h6/7L from SIVmac239	h4/5L and h6/7L from SIVmac239 and Q110D
Binding energy (kcal/mol)	-64.447	-31.012	-36.071	-30.051

Fig. 6. Structural models of HIV CA NTD bound to CypA. The model of CA NTD bound to CypA was constructed by homology modeling using the crystal structure of HIV-1 CA NTD and CypA complex (PDB code: 1M9C [28]). The binding energies, E_{bind} (kcal/mol), of the complex were calculated using MOE as described previously [42,43]. The formula $E_{bind} = E_{complex} - (E_{CA} + E_{CypA})$ was used for the E_{bind} calculation, where $E_{complex}$ is the energy of the CA/CypA complex models, E_{CA} is the energy of the CA monomer model, and E_{CypA} is the energy of the CypA monomer model.

domain [46]. Thus, it is not unreasonable to assume that the replication of MN4Rh-3 carrying CA-Q110D is enhanced in macaque cells but reduced in human cells by augmenting its dissociation from CypA (Fig. 6). However, it was found to be difficult to experimentally confirm this structural insight by determining the effect of cyclosporine A or of siRNA against CypA on viral infectivity because interaction between the HIV-1mt CA and CypA was so weak. Alternatively, CA-Q110D may contribute to the alteration of the affinity to unknown anti-CA factor(s) other than CypA and TRIM5 proteins. In this case, it is speculated that the factor(s) might act negatively on HIV-1 replication in macaque cells but positively in human cells, and vice versa. Further study is required to elucidate the mechanism for enhancement of viral growth potential by CA-Q110D.

In conclusion, further modification of the HIV-1mt genome is necessary to overcome unconquered replication block(s) present in macaque cells and obtain viral clones similarly replication-competent in macaque cells and pathogenic for animals with SIVmac (Fig. 5). Considering the genome structure of MN4Rh-3 and the results presented here, major targets for modification now are *gag*-CA (against TRIM5α) and *vpu* (against tetherin). Gag-CA is one of the two principal viral determinants (CA and Vif) for the HIV-1 species-tropism. Construction of HIV-1 CA that evades from TRIM5α restriction is also useful for elucidation of the less-defined CA-TRIM5α interaction and antiviral mechanism of TRIM5α. Tetherin, identified as anti-virion release factor, is antagonized by Vpu [47,48], but macaque tetherin was not counteracted by HIV-1 Vpu [49]. Construction of HIV-1 Vpu that down-modulate macaque tetherin may enhance viral replication *in vivo* as well as *in vitro* [50]. Through these approaches, we may be able to precisely analyze HIV-1 replication and pathogenesis *in vivo* and provide new strategies against HIV-1/AIDS.

Acknowledgments

This study was supported by a grant from the Ministry of Health, Labor and Welfare of Japan (Research on HIV/AIDS project no. H23-003).

References

[1] M.H. Malim, M. Emerman, HIV-1 accessory proteins–ensuring viral survival in a hostile environment, Cell Host Microbe 3 (2008) 388–398.
[2] F. Kirchhoff, Immune evasion and counteraction of restriction factors by HIV-1 and other primate lentiviruses, Cell Host Microbe 8 (2010) 55–67.
[3] R. Shibata, H. Sakai, M. Kawamura, K. Tokunaga, A. Adachi, Early replication block of human immunodeficiency virus type 1 in monkey cells, J. Gen. Virol. 76 (1995) 2723–2730.
[4] M. Nomaguchi, N. Doi, K. Kamada, A. Adachi, Species barrier of HIV-1 and its jumping by virus engineering, Rev. Med. Virol. 18 (2008) 261–275.
[5] M. Nomaguchi, A. Adachi, Virology as biosystematics: towards understanding the viral infection biology, Front. Microbiol. 1 (2010) 2.
[6] R.K. Holmes, M.H. Malim, K.N. Bishop, APOBEC-mediated viral restriction: not simply editing? Trends Biochem. Sci. 32 (2007) 118–128.
[7] H. Huthoff, G.J. Towers, Restriction of retroviral replication by APOBEC3G/F and TRIM5alpha, Trends Microbiol. 16 (2008) 612–619.
[8] K. Strebel, J. Luban, K.T. Jeang, Human cellular restriction factors that target HIV-1 replication, BMC Med. 7 (2009) 48.
[9] J. Luban, Cyclophilin A, TRIM5, and resistance to human immunodeficiency virus type 1 infection, J. Virol. 81 (2007) 1054–1061.
[10] G.J. Towers, The control of viral infection by tripartite motif proteins and cyclophilin A, Retrovirology 4 (2007) 40.
[11] E.E. Nakayama, T. Shioda, Anti-retroviral activity of TRIM5 alpha, Rev. Med. Virol. 20 (2010) 77–92.
[12] R.M. Newman, L. Hall, M. Connole, G.L. Chen, S. Sato, E. Yuste, W. Diehl, E. Hunter, A. Kaur, G.M. Miller, W.E. Johnson, Balancing selection and the evolution of functional polymorphism in old world monkey TRIM5alpha, Proc. Natl. Acad. Sci. U. S. A. 103 (2006) 19134–19139.
[13] S.J. Wilson, B.L. Webb, L.M. Ylinen, E. Verschoor, J.L. Heeney, G.J. Towers, Independent evolution of an antiviral TRIMCyp in rhesus macaques, Proc. Natl. Acad. Sci. U. S. A. 105 (2008) 3557–3562.

[14] A.J. Price, F. Marzetta, M. Lammers, L.M. Ylinen, T. Schaller, S.J. Wilson, G.J. Towers, L.C. James, Active site remodeling switches HIV specificity of antiretroviral TRIMCyp, Nat. Struct. Mol. Biol. 16 (2009) 1036–1042.

[15] L.M. Ylinen, A.J. Price, J. Rasaiyaah, S. Hué, N.J. Rose, F. Marzetta, L.C. James, G.J. Towers, Conformational adaptation of Asian macaque TRIMCyp directs lineage specific antiviral activity, PLoS Pathog. 6 (2010) e1001062.

[16] K. Kamada, T. Igarashi, M.A. Martin, B. Khamsri, K. Hatcho, T. Yamashita, M. Fujita, T. Uchiyama, A. Adachi, Generation of HIV-1 derivatives that productively infect macaque monkey lymphoid cells, Proc. Natl. Acad. Sci. U. S. A. 103 (2006) 16959–16964.

[17] T. Igarashi, R. Iyengar, R.A. Byrum, A. Buckler-White, R.L. Dewar, C.E. Buckler, H.C. Lane, K. Kamada, A. Adachi, M.A. Martin, Human immunodeficiency virus type 1 derivative with 7% simian immunodeficiency virus genetic content is able to establish infections in pig-tailed macaques, J. Virol. 81 (2007) 11549–11552.

[18] K. Kamada, T. Yamashita, K. Hatcho, A. Adachi, M. Nomaguchi, Evasion from CypA- and APOBEC-mediated restrictions is insufficient for HIV-1 to efficiently grow in simian cells, Microbes Infect. 11 (2009) 164–171.

[19] A. Saito, M. Nomaguchi, S. Iijima, A. Kuroishi, T. Yoshida, Y.J. Lee, T. Hayakawa, K. Kono, E.E. Nakayama, T. Shioda, Y. Yasutomi, A. Adachi, T. Matano, H. Akari, Improved capacity of a monkey-tropic HIV-1 derivative to replicate in cynomolgus monkeys with minimal modifications, Microbes Infect. 13 (2011) 58–64.

[20] A. Kuroishi, A. Saito, Y. Shingai, T. Shioda, M. Nomaguchi, A. Adachi, H. Akari, E.E. Nakayama, Modification of a loop sequence between alpha-helices 6 and 7 of virus capsid (CA) protein in a human immunodeficiency virus type 1 (HIV-1) derivative that has simian immunodeficiency virus (SIVmac239) vif and CA alpha-helices 4 and 5 loop improves replication in cynomolgus monkey cells, Retrovirology 6 (2009) 70.

[21] T. Yamashita, N. Doi, A. Adachi, M. Nomaguchi, Growth ability in simian cells of monkey cell-tropic HIV-1 is greatly affected by downstream region of the vif gene, J. Med. Invest. 55 (2008) 236–240.

[22] M. Yamashita, M. Emerman, Capsid is a dominant determinant of retrovirus infectivity in nondividing cells, J. Virol. 78 (2004) 5670–5678.

[23] J.S. Lebkowski, S. Clancy, M.P. Calos, Simian virus 40 replication in adenovirus-transformed human cells antagonizes gene expression, Nature 317 (1985) 169–171.

[24] H. Akari, T. Fukumori, S. Iida, A. Adachi, Induction of apoptosis in herpesvirus saimiri-immortalized T lymphocytes by blocking interaction of CD28 with CD80/CD86, Biochem. Biophys. Res. Commun. 263 (1999) 352–356.

[25] N. Doi, S. Fujiwara, A. Adachi, M. Nomaguchi, Growth ability in various macaque cell lines of HIV-1 with simian cell-tropism, J. Med. Invest. 57 (2010) 284–292.

[26] A. Adachi, H.E. Gendelman, S. Koenig, T. Folks, R. Willey, A. Rabson, M.A. Martin, Production of acquired immunodeficiency syndrome-associated retrovirus in human and nonhuman cells transfected with an infectious molecular clone, J. Virol. 59 (1986) 284–291.

[27] U. O'Doherty, W.J. Swiggard, M.H. Malim, Human immunodeficiency virus type 1 spinoculation enhances infection through virus binding, J. Virol. 74 (2004) 10074–10080.

[28] B.R. Howard, F.F. Vajdos, S. Li, W.I. Sundquist, C.P. Hill, Structural insights into the catalytic mechanism of cyclophilin A, Nat. Struct. Biol. 10 (2003) 475–481.

[29] N. Deshpande, K.J. Addess, W.F. Bluhm, J.C. Merino-Ott, W. Townsend-Merino, Q. Zhang, C. Knezevich, L. Xie, L. Chen, Z. Feng, R.K. Green, J.L. Flippen-Anderson, J. Westbrook, H.M. Berman, P.E. Bourne, The RCSB protein data bank: a redesigned query system and relational database based on the mmCIF schema, Nucleic Acids Res. 33 (Database issue) (2005) D233–D237.

[30] H. Song, E.E. Nakayama, M. Yokoyama, H. Sato, J.A. Levy, T. Shioda, A single amino acid of the human immunodeficiency virus type 2 capsid affects its replication in the presence of cynomolgus monkey and human TRIM5alphas, J. Virol. 81 (2007) 7280–7285.

[31] K. Kono, H. Song, M. Yokoyama, H. Sato, T. Shioda, E.E. Nakayama, Multiple sites in the N-terminal half of simian immunodeficiency virus capsid protein contribute to evasion from rhesus monkey TRIM5α-mediated restriction, Retrovirology 7 (2010) 72.

[32] N. Inagaki, H. Takeuchi, M. Yokoyama, H. Sato, A. Ryo, H. Yamamoto, M. Kawada, T. Matano, A structural constraint for functional interaction between N-terminal and C-terminal domains in simian immunodeficiency virus capsid proteins, Retrovirology 7 (2010) 90.

[33] P. Labute, The generalized Born/volume integral implicit solvent model: estimation of the free energy of hydration using London dispersion instead of atomic surface area, J. Comput. Chem. 29 (2008) 1693–1698.

[34] J.W. Ponder, D.A. Case, Force fields for protein simulations, Adv. Protein Chem. 66 (2003) 27–85.

[35] A. Onufriev, D. Bashford, D.A. Case, Modification of the generalized Born model suitable for macromolecules, J. Phys. Chem. B 104 (2000) 3712–3720.

[36] T.Y. Lin, M. Emerman, Determinants of cyclophilin A-dependent TRIM5 alpha restriction against HIV-1, Virology 379 (2008) 335–341.

[37] A. Kuroishi, K. Bozek, T. Shioda, E.E. Nakayama, A single amino acid substitution of the human immunodeficiency virus type 1 capsid protein affects viral sensitivity to TRIM5 alpha, Retrovirology 7 (2010) 58.

[38] M. Stremlau, C.M. Owens, M.J. Perron, M. Kiessling, P. Autissier, J. Sodroski, The cytoplasmic body component TRIM5alpha restricts HIV-1 infection in old world monkeys, Nature 427 (2004) 848–853.

[39] Z. Keckesova, L.M. Ylinen, G.J. Towers, Cyclophilin A renders human immunodeficiency virus type 1 sensitive to old world monkey but not human TRIM5 alpha antiviral activity, J. Virol. 80 (2006) 4683–4690.

[40] E. Sokolskaja, L. Berthoux, J. Luban, Cyclophilin A and TRIM5alpha independently regulate human immunodeficiency virus type 1 infectivity in human cells, J. Virol. 80 (2006) 2855–2862.

[41] S.Y. Lim, T. Rogers, T. Chan, J.B. Whitney, J. Kim, J. Sodroski, N.L. Letvin, TRIM5alpha modulates immunodeficiency virus control in rhesus monkeys, PLoS Pathog. 6 (2010) e1000738.

[42] C.O. Onyango, A. Leligdowicz, M. Yokoyama, H. Sato, H. Song, E.E. Nakayama, T. Shioda, T. de Silva, J. Townend, A. Jaye, H. Whittle, S. Rowland-Jones, M. Cotten, HIV-2 capsids distinguish high and low virus load patients in a West African community cohort, Vaccine 28 (2010) B60–B67.

[43] M. Kinomoto, R. Appiah-Opong, J.A. Brandful, M. Yokoyama, N. Nii-Trebi, E. Ugly-Kwame, H. Sato, D. Ofori-Adjei, T. Kurata, F. Barre-Sinoussi, T. Sata, K. Tokunaga, HIV-1 proteases from drug-naive West African patients are differentially less susceptible to protease inhibitors, Clin. Infect. Dis. 41 (2005) 243–251.

[44] R.K. Gitti, B.M. Lee, J. Walker, M.F. Summers, S. Yoo, W.I. Sundquist, Structure of the amino-terminal core domain of the HIV-1 capsid protein, Science 273 (1996) 231–235.

[45] C. Tang, Y. Ndassa, M.F. Summers, Structure of the N-terminal 283-residue fragment of the immature HIV-1 Gag polyprotein, Nat. Struct. Biol. 9 (2002) 537–543.

[46] M. Yokoyama, S. Naganawa, K. Yoshimura, S. Matsushita, H. Sato, Structural dynamics of HIV-1 envelope Gp120 outer domain with V3 loop, PLoS One 7 (2012) e37530.

[47] S.J. Neil, T. Zang, P.D. Bieniasz, Tetherin inhibits retrovirus release and is antagonized by HIV-1 Vpu, Nature 451 (2008) 425–430.

[48] N. Van Damme, D. Goff, C. Katsura, R.L. Jorgenson, R. Mitchell, M.C. Johnson, E.B. Stephens, J. Guatelli, The interferon-induced protein BST-2 restricts HIV-1 release and is downregulated from the cell surface by the viral Vpu protein, Cell Host Microbe 3 (2008) 245–252.

[49] D. Sauter, M. Schindler, A. Specht, W.N. Landford, J. Münch, K.A. Kim, J. Votteler, U. Schubert, F. Bibollet-Ruche, B.F. Keele, J. Takehisa, Y. Ogando, C. Ochsenbauer, J.C. Kappes, A. Ayouba, M. Peeters, G.H. Learn, G. Shaw, P.M. Sharp, P. Bieniasz, B.H. Hahn, T. Hatziioannou, F. Kirchhoff, Tetherin-driven adaptation of Vpu and Nef function and the evolution of pandemic and nonpandemic HIV-1 strains, Cell Host Microbe 6 (2009) 409–421.

[50] M. Shingai, T. Yoshida, M.A. Martin, K. Strebel, Some human immunodeficiency virus type 1 Vpu proteins are able to antagonize macaque BST-2 in vitro and in vivo: Vpu-negative simian-human immunodeficiency viruses are attenuated in vivo, J. Virol. 85 (2011) 9708–9715.

frontiers in
MICROBIOLOGY

MINI REVIEW ARTICLE
published: 13 October 2011
doi: 10.3389/fmicb.2011.00210

Non-enzymatic functions of retroviral integrase: the next target for novel anti-HIV drug development

Takao Masuda*

Department of Immunotherapeutics, Tokyo Medical and Dental University, Tokyo, Japan

Edited by:
Akio Adachi, The University of Tokushima Graduate School, Japan

Reviewed by:
Mikako Fujita, Kumamoto University, Japan
Yasuyuki Miyazaki, The University of Tokushima Graduate School, Japan

***Correspondence:**
Takao Masuda, Department of Immunotherapeutics, Graduate School of Medicine and Dentistry, Tokyo Medical and Dental University, 1-5-45 Yushima, Bunkyo-ku, Tokyo 113-8519, Japan.
e-mail: tmasu.impt@tmd.ac.jp

Integrase (IN) is a retroviral enzyme that catalyzes the insertion of viral DNA (vDNA) into host chromosomal DNA, which is necessary for efficient viral replication. The crystal structure of prototype foamy virus IN bound to cognate vDNA ends, a complex referred to as the intasome, has recently been resolved. Structure analysis of the intasome revealed a tetramer structure of IN that was required for its catalytic function, and also showed the inhibitory mechanism of the IN inhibitor. Genetic analysis of IN has revealed additional non-enzymatic roles during viral replication cycles at several steps other than integration. However, the higher order structure of IN that is required for its non-enzymatic functions remains to be delineated. This is the next major challenge in the field of IN structural biology hoping to be a platform for the development of novel IN inhibitors to treat human immunodeficiency virus type 1 infectious disease.

Keywords: HIV-1, integrase, reverse transcriptase, *pol*, reverse transcription, intasome, Gemin2

INTRODUCTION

Reverse transcription of viral RNA into double-stranded (ds) DNA, and the subsequent insertion of the synthesized viral DNA (vDNA) into a host chromosome, are characteristic features of retroviruses including human immunodeficiency virus type 1 (HIV-1). The reverse transcription and integration of the viral genome is sequentially catalyzed by the enzymes reverse transcriptase (RT) and integrase (IN), respectively. These retroviral enzymes are originally packaged in the viral particle along with the viral genomic RNA. After synthesis of vDNA by RT, IN acts on the termini of vDNA and catalyzes insertion of the vDNA into the host chromosome through two sequential enzymatic reactions: 3′-end processing and strand-transfer (Katz and Skalka, 1994). Currently, a clinically approved IN inhibitor specifically targets strand-transfer activity but not 3′-end processing activity (Summa et al., 2008). Therefore, the IN inhibitor is referred to as a strand-transfer inhibitor (STI). The STI shows very potent antiviral activity; however, emergence of STI-resistant variants is inevitable (Metifiot et al., 2010), as seen in patients treated with a combination of inhibitors against RT and protease activities. Efforts to develop novel drugs with distinct inhibitory mechanisms must continue so that we can effectively treat HIV-1 infections. For development of novel IN inhibitors, in addition to its enzymatic action, other non-enzymatic functions of IN, as described below, might be the next target(s) (Luo and Muesing, 2010).

STRUCTURE OF HIV-1 IN

Human immunodeficiency virus type 1 IN is composed of 288 amino acids with three structurally distinct domains (Li et al., 2011): an N-terminal domain (NTD), a central catalytic core domain (CCD), and a C-terminal domain (CTD; **Figure 1**). The NTD contains a highly conserved (His-His-Cys-Cys, HHCC) motif, which binds to zinc ions (Zn^{2+}) and folds a helix-turn-helix (HTH) structure. Through a tetrahedral attachment to the HHCC motif, Zn^{2+} enhances both multimerization and enzymatic activities of HIV-1 IN *in vitro* (Burke et al., 1992; Ellison et al., 1995; Cai et al., 1997). The CCD contains the highly conserved Asp, Asp, and Glu (DDE) residues directly involved in the catalytic activities of IN (Engelman and Craigie, 1992; Kulkosky et al., 1992; LaFemina et al., 1992; Bushman et al., 1993). Overall topology of the CCD is similar to those of ribonuclease H (RNaseH), the Holliday junction resolvase RuvC, and bacteriophage transposase Mu. Despite lack of sequence similarity between the CCD and RNaseH, there is remarkable similarity in the positioning of the two Asp catalytic residues (Dyda et al., 1994). The CTD, consisting of a structure that closely resembles Src homology 3 domains (SH3-like), possesses sequence- and metal ion-independent DNA binding activity (Eijkelenboom et al., 1995; Lodi et al., 1995). Each domain has been demonstrated to form a dimer and higher multimerization states (Dyda et al., 1994; Eijkelenboom et al., 1995; Cai et al., 1997), which might be required for all the enzymatic functions of IN.

Recently, the entire prototype foamy virus (PFV) IN in a complex with its cognate vDNA ends, referred to as the intasome, has been successfully crystallized (Hare et al., 2010). The crystal structure analysis of the PFV intasome revealed an unprecedented tetramer structure for IN (see Cherepanov et al., 2011; Li et al., 2011 for recent review). The IN tetramer structure observed in the PFV intasome demonstrated that two sets of IN dimer acts on each vDNA end (**Figure 2**). The inner subunits of each IN dimer contact with vDNA and form a tetramer. The outer subunits of each IN dimer might be speculated to have supportive or other functions, such as engagement of target DNA or interaction with host factors. Several models for the IN tetramer have been proposed from previous structure analysis using partial IN fragments possessing the NTD–CCD or CCD–CTD (Chen et al., 2000; Wang et al., 2001;

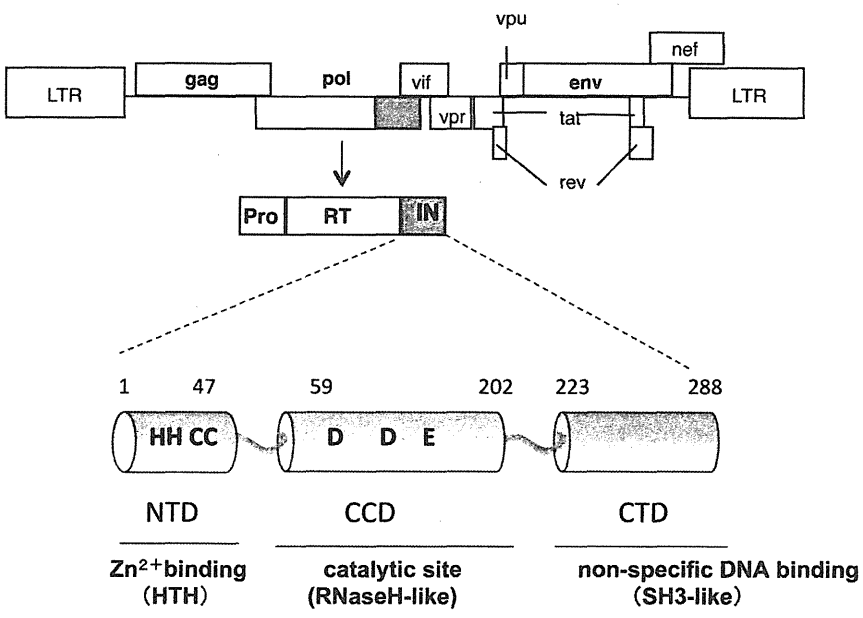

FIGURE 1 | Schematic diagram of HIV-1 IN. The genetic organization of HIV-1 is shown at the top. HIV-1 IN is encoded by the pol region and composed of 288 amino acids with three structurally distinct domains: an N-terminal domain (NTD); a central catalytic core domain (CCD); and a C-terminal domain (CTD). The CCD contains the highly conserved DDE motif, which is directly involved in the catalytic activities of IN. Overall topology of the CCD is similar to that of ribonuclease H (RNaseH). The NTD, contains a highly conserved HHCC motif, which binds to zinc and folds a helix-turn-helix (HTH) structure. The CTD, consisting of a structure that closely resembles Src homology 3 domains (SH3), possesses sequence- and metal ion-independent DNA binding activity.

Hare et al., 2009a). However, these IN tetramer models are different from those observed in the active PFV intasome (Craigie, 2010). Stable interaction of IN with 3′-end processed vDNA in the intasome might be a plausible explanation for the difference. The stable IN tetramer formation observed in the intasome reflects the IN-DNA complex required for proper concerted integration of both vDNA ends into the proximal sites of the target host chromosomal DNA. Furthermore, analysis of the PFV intasome interacting with the STI elucidated its inhibitory mechanism. Based on the PFV intasome structure as a template, structural modeling of the HIV-1 intasome has also been reported (Krishnan et al., 2010). Structural analysis of this intasome revealed numerous details of retroviral integration and will contribute to the design of the next generation of HIV-1 IN catalytic inhibitors. The functional significance of the DNA-independent IN tetramer as observed by analysis of partial IN fragments (Chen et al., 2000; Wang et al., 2001; Hare et al., 2009a) remains unclear (Cherepanov et al., 2011).

NON-ENZYMATIC FUNCTIONS OF IN

Originally, we found that introduction of amino acid substitutions at conserved HHCC residues in the NTD of HIV-1 IN resulted in almost complete abrogation of proviral DNA formation, concomitant with a severe reduction in vDNA synthesis. This suggests the mutations in the IN affected the viral life cycle at steps prior to integration (Masuda et al., 1995). Further genetic analysis of HIV-1 IN revealed that the pleiotropic effects of IN mutations affected uncoating (Masuda et al., 1995; Leavitt et al., 1996; Nakamura et al., 1997; Briones et al., 2010), reverse transcription (Engelman et al., 1995; Masuda et al., 1995; Wu et al., 1999; Tsurutani et al., 2000; Nishitsuji et al., 2009) nuclear import of vDNA (Gallay et al., 1997; Tsurutani et al., 2000; Ikeda et al., 2004), and protein processing during viral particle assembly and maturation (Mohammed et al., 2011). Importantly, HIV-1 carrying point mutations at the catalytic sites of IN (DDE) affected the integration step, but not vDNA synthesis (Masuda et al., 1995). Thus, the pleiotropic effects of IN mutations might not be directly related to the loss of its catalytic function. These experiments suggest that IN may possess non-enzymatic roles throughout the viral replication cycle (**Figure 2**).

Among the possible non-enzymatic roles of IN, there has been an accumulation of evidence to suggest involvement of retroviral IN during reverse transcription (Engelman et al., 1995; Masuda et al., 1995; Tsurutani et al., 2000; Lu et al., 2005; Dobard et al., 2007). The contribution of IN during reverse transcription has also been noticed in a retrovirus-like element of *Saccharomyces cerevisiae*, Ty3 (Nymark-McMahon and Sandmeyer, 1999; Nymark-McMahon et al., 2002). A previous study from our laboratory showed that reverse transcription of HIV-1 was abrogated by knocking down a host factor, survival motor neuron (SMN)-interacting protein 1 (SIP1/Gemin2), which binds to HIV-1 IN (Hamamoto et al., 2006). Gemin 2 is a component of the SMN complex that mediates the assembly of spliceosomal small nuclear ribonucleoproteins and nucleolar ribonucleoproteins (Fischer et al., 1997; Liu et al., 1997; Buhler et al., 1999; Jablonka et al., 2001; Meister et al., 2001). In a subsequent study, we demonstrated that HIV-1 IN and Gemin2 synergistically stimulate

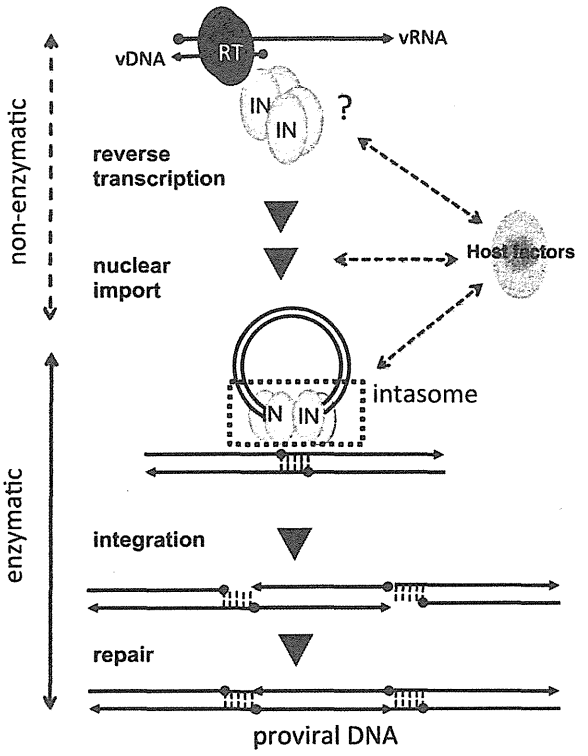

FIGURE 2 | Non-enzymatic and enzymatic roles of HIV-1 IN that help establish proviral DNA. After entry into cells, retroviral genomic RNA (vRNA) is reverse transcribed into DNA (vDNA) by RT. Then, vDNA is transported into the nucleus (nuclear import) and finally integrated into host chromosomal DNA (black lines). IN forms a functional tetramer with vDNA ends (intasome) to assist with integration. Subsequent repair processes by host DNA repair machinery establishes the proviral DNA, in which retrovirus DNA is stably integrated into host chromosomal DNA. IN tetramer structures for its enzymatic (integration) and non-enzymatic functions (reverse transcription and nuclear import) and possible involvement of host factors are schematically depicted. The vRNA, vDNA, and host DNA are shown as blue, red, and black lines, respectively. An arrowhead shows the direction of each genome from the 5′- to the 3′-end.

RT activity by enhancing the assembly of RT on viral RNA *in vitro* (Nishitsuji et al., 2009). Chow and colleagues have also reported that HIV-1 IN stimulates RT activity through physical interactions with RT (Zhu et al., 2004). Thus, IN might possess a direct function to support efficient reverse transcription by RT.

INSIGHT ON PUTATIVE STRUCTURE OF IN FOR ITS NON-ENZYMATIC FUNCTION

Delineation of the IN mutant structure could provide clues for depicting the IN conformation required for non-enzymatic functions. Nuclear magnetic resonance (NMR) analysis of an isolated NTD has shown that the NTD exists in two conformational states, the E and D forms (Cai et al., 1997). A previous study using NMR spectroscopy indicated that the NTD mutant protein, in which the Tyr 15 residue was replaced with Ala (Y15A), folds correctly but only as the E form (Nomura et al., 2006). The IN tetramer structure was formed through interaction of NTD–CCD between the inner subunits in the intasome (Hare et al., 2010). The residues 13–26 and 40–45 in the NTD interact extensively with residues 150–196 in the CCD of the other subunit. The importance of the NTD–CCD interaction to form the IN tetramer has been proposed from previous crystal structure analysis using the NTD–CCD IN fragments (Wang et al., 2001; Hare et al., 2009b). As observed in these previous analyses, the hydrogen-bond contacts between the side chains of CCD residues Gln164 and Arg187 and the backbones of the NTD residues Lys14 and Tyr15 also persist in the recent structure-based model of the HIV-1 IN intasome (Krishnan et al., 2010). HIV-1 carrying IN mutations at the Lys186, Arg187, and Lys188 residues exhibited a reverse transcription-defective phenotype (Tsurutani et al., 2000) as found in the NTD mutants including Y15A. These experimental data suggest that the functional tetramer form, stabilized with the NTD–CCD interaction, might be critical for the non-enzymatic function of IN during reverse transcription.

IMPACT OF HOST FACTORS ON IN STRUCTURE AND NON-ENZYMATIC FUNCTION

Numerous host factors that interact with HIV-1 IN have been reported (Al-Mawsawi and Neamati, 2007). The best characterized factor is lens epithelium-derived growth factor/transcription co-activator p75 (LEDGF/p75; Cherepanov et al., 2003) for chromosomal targeting of HIV-1 IN (Maertens et al., 2003, 2004; Shun et al., 2007). The crystal structure analysis of the PFV intasome (Hare et al., 2010) together with results from previous studies (Li et al., 2006; Hare et al., 2009a) suggest that synapsis formation with DNA ends of the virus through tetramerization of IN might be critical for proper assembly and/or a stable and functionally active intasome. Importantly, LEDGF/p75 stabilizes the functional tetramer of IN for its enzymatic function. Meanwhile, a reduction of the tetramer form of IN was reproduced when wild-type IN was expressed in cells in which endogenous Gemin2 was knocked down by RNA interference (Nishitsuji et al., 2009). We also noticed that the intracellular stability and multimer formation of IN, especially the tetramer formation of IN, were dramatically reduced by IN mutations that led to a reverse transcription-defective phenotype. Thus, in the absence of vDNA, host factors might be involved in forming or maintaining highly ordered structures of IN, which is critical for non-enzymatic function. Therefore, inhibition of the interaction between IN and host factors could be a novel therapeutic approach for the design and development of new classes of IN inhibitors targeting non-enzymatic functions.

CONCLUSION

It is obvious that IN must be closely associated with the viral genome complex to form an active intasome upon the completion of reverse transcription. Physical interaction of IN with RT (Zhu et al., 2004; Wilkinson et al., 2009) could contribute to keeping IN close to the viral genome complex. How is the IN structure in the absence of vDNA before and during reverse transcription maintained? What is the contribution of host factors to

IN conformation that is required for non-enzymatic functions? The highly ordered IN structure and/or its interface structure for interaction with host factors required for non-enzymatic IN function(s) should be determined.

Finally, it should be emphasized that IN mutations affecting non-enzymatic function resulted in severe deleterious affects to HIV-1 replication compared with IN mutations that specifically affected catalytic activity. Clinical efficacy of the STI that blocks IN catalytic activity guarantees that a greater impact on HIV-1 control would be achieved with a novel inhibitor that blocks the non-enzymatic function of IN.

ACKNOWLEDGMENTS

This work was supported by a Grant-in-Aid for Scientific Research on Priority Areas from the Ministry of Education, Culture, Sports, Science, and Technology (MEXT) of Japan and a grant for HIV/AIDS research from the Ministry of Health, Labor, and Welfare of Japan.

REFERENCES

Al-Mawsawi, L. Q., and Neamati, N. (2007). Blocking interactions between HIV-1 integrase and cellular cofactors: an emerging antiretroviral strategy. *Trends Pharmacol. Sci.* 28, 526–535.

Briones, M. S., Dobard, C. W., and Chow, S. A. (2010). Role of human immunodeficiency virus type 1 integrase in uncoating of the viral core. *J. Virol.* 84, 5181–5190.

Buhler, D., Raker, V., Luhrmann, R., and Fischer, U. (1999). Essential role for the tudor domain of SMN in spliceosomal U snRNP assembly: implications for spinal muscular atrophy. *Hum. Mol. Genet.* 8, 2351–2357.

Burke, C. J., Sanyal, G., Bruner, M. W., Ryan, J. A., Lafemina, R. L., Robbins, H. L., Zeft, A. S., Middaugh, C. R., and Cordingley, M. G. (1992). Structural implications of spectroscopic characterization of a putative zinc finger peptide from HIV-1 integrase. *J. Biol. Chem.* 267, 9639–9644.

Bushman, F. D., Engelman, A., Palmer, I., Wingfield, P., and Craigie, R. (1993). Domains of the integrase protein of human immunodeficiency virus type 1 responsible for polynucleotidyl transfer and zinc binding. *Proc. Natl. Acad. Sci. U.S.A.* 90, 3428–3432.

Cai, M., Zheng, R., Caffrey, M., Craigie, R., Clore, G. M., and Gronenborn, A. M. (1997). Solution structure of the N-terminal zinc binding domain of HIV-1 integrase. *Nat. Struct. Biol.* 4, 567–577.

Chen, J. C., Krucinski, J., Miercke, L. J., Finer-Moore, J. S., Tang, A. H., Leavitt, A. D., and Stroud, R. M. (2000). Crystal structure of the HIV-1 integrase catalytic core and C-terminal domains: a model for viral DNA binding. *Proc. Natl. Acad. Sci. U.S.A.* 97, 8233–8238.

Cherepanov, P., Maertens, G., Proost, P., Devreese, B., Van Beeumen, J., Engelborghs, Y., De Clercq, E., and Debyser, Z. (2003). HIV-1 integrase forms stable tetramers and associates with LEDGF/p75 protein in human cells. *J. Biol. Chem.* 278, 372–381.

Cherepanov, P., Maertens, G. N., and Hare, S. (2011). Structural insights into the retroviral DNA integration apparatus. *Curr. Opin. Struct. Biol.* 21, 249–256.

Craigie, R. (2010). Structural biology: when four become one. *Nature* 464, 167–168.

Dobard, C. W., Briones, M. S., and Chow, S. A. (2007). Molecular mechanisms by which human immunodeficiency virus type 1 integrase stimulates the early steps of reverse transcription. *J. Virol.* 81, 10037–10046.

Dyda, F., Hickman, A. B., Jenkins, T. M., Engelman, A., Craigie, R., and Davies, D. R. (1994). Crystal structure of the catalytic domain of HIV-1 integrase: similarity to other polynucleotidyl transferases. *Science* 266, 1981–1986.

Eijkelenboom, A. P., Lutzke, R. A., Boelens, R., Plasterk, R. H., Kaptein, R., and Hard, K. (1995). The DNA-binding domain of HIV-1 integrase has an SH3-like fold. *Nat. Struct. Biol.* 2, 807–810.

Ellison, V., Gerton, J., Vincent, K. A., and Brown, P. O. (1995). An essential interaction between distinct domains of HIV-1 integrase mediates assembly of the active multimer. *J. Biol. Chem.* 270, 3320–3326.

Engelman, A., and Craigie, R. (1992). Identification of conserved amino acid residues critical for human immunodeficiency virus type 1 integrase function in vitro. *J. Virol.* 66, 6361–6369.

Engelman, A., Englund, G., Orenstein, J. M., Martin, M. A., and Craigie, R. (1995). Multiple effects of mutations in human immunodeficiency virus type 1 integrase on viral replication. *J. Virol.* 69, 2729–2736.

Fischer, U., Liu, Q., and Dreyfuss, G. (1997). The SMN-SIP1 complex has an essential role in spliceosomal snRNP biogenesis. *Cell* 90, 1023–1029.

Gallay, P., Hope, T., Chin, D., and Trono, D. (1997). HIV-1 infection of nondividing cells through the recognition of integrase by the importin/karyopherin pathway. *Proc. Natl. Acad. Sci. U.S.A.* 94, 9825–9830.

Hamamoto, S., Nishitsuji, H., Amagasa, T., Kannagi, M., and Masuda, T. (2006). Identification of a novel human immunodeficiency virus type 1 integrase interactor, Gemin2, that facilitates efficient viral cDNA synthesis in vivo. *J. Virol.* 80, 5670–5677.

Hare, S., Di Nunzio, F., Labeja, A., Wang, J., Engelman, A., and Cherepanov, P. (2009a). Structural basis for functional tetramerization of lentiviral integrase. *PLoS Pathog.* 5, e1000515. doi:10.1371/journal.ppat.1000515

Hare, S., Shun, M. C., Gupta, S. S., Valkov, E., Engelman, A., and Cherepanov, P. (2009b). A novel co-crystal structure affords the design of gain-of-function lentiviral integrase mutants in the presence of modified PSIP1/LEDGF/p75. *PLoS Pathog.* 5, e1000259. doi:10.1371/journal.ppat.1000259

Hare, S., Gupta, S. S., Valkov, E., Engelman, A., and Cherepanov, P. (2010). Retroviral intasome assembly and inhibition of DNA strand transfer. *Nature* 464, 232–236.

Ikeda, T., Nishitsuji, H., Zhou, X., Nara, N., Ohashi, T., Kannagi, M., and Masuda, T. (2004). Evaluation of the functional involvement of human immunodeficiency virus type 1 integrase in nuclear import of viral cDNA during acute infection. *J. Virol.* 78, 11563–11573.

Jablonka, S., Bandilla, M., Wiese, S., Buhler, D., Wirth, B., Sendtner, M., and Fischer, U. (2001). Co-regulation of survival of motor neuron (SMN) protein and its interactor SIP1 during development and in spinal muscular atrophy. *Hum. Mol. Genet.* 10, 497–505.

Katz, R. A., and Skalka, A. M. (1994). The retroviral enzymes. *Annu. Rev. Biochem.* 63, 133–173.

Krishnan, L., Li, X., Naraharisetty, H. L., Hare, S., Cherepanov, P., and Engelman, A. (2010). Structure-based modeling of the functional HIV-1 intasome and its inhibition. *Proc. Natl. Acad. Sci. U.S.A.* 107, 15910–15915.

Kulkosky, J., Jones, K. S., Katz, R. A., Mack, J. P., and Skalka, A. M. (1992). Residues critical for retroviral integrative recombination in a region that is highly conserved among retroviral/retrotransposon integrases and bacterial insertion sequence transposases. *Mol. Cell. Biol.* 12, 2331–2338.

LaFemina, R. L., Schneider, C. L., Robbins, H. L., Callahan, P. L., Legrow, K., Roth, E., Schleif, W. A., and Emini, E. A. (1992). Requirement of active human immunodeficiency virus type 1 integrase enzyme for productive infection of human T-lymphoid cells. *J. Virol.* 66, 7414–7419.

Leavitt, A. D., Robles, G., Alesandro, N., and Varmus, H. E. (1996). Human immunodeficiency virus type 1 integrase mutants retain in vitro integrase activity yet fail to integrate viral DNA efficiently during infection. *J. Virol.* 70, 721–728.

Li, M., Mizuuchi, M., Burke, T. R. Jr., and Craigie, R. (2006). Retroviral DNA integration: reaction pathway and critical intermediates. *EMBO J.* 25, 1295–1304.

Li, X., Krishnan, L., Cherepanov, P., and Engelman, A. (2011). Structural biology of retroviral DNA integration. *Virology* 411, 194–205.

Liu, Q., Fischer, U., Wang, F., and Dreyfuss, G. (1997). The spinal muscular atrophy disease gene product, SMN, and its associated protein SIP1 are in a complex with spliceosomal snRNP proteins. *Cell* 90, 1013–1021.

Lodi, P. J., Ernst, J. A., Kuszewski, J., Hickman, A. B., Engelman, A., Craigie, R., Clore, G. M., and Gronenborn, A. M. (1995). Solution structure of the DNA binding domain of HIV-1 integrase. *Biochemistry* 34, 9826–9833.

Lu, R., Ghory, H. Z., and Engelman, A. (2005). Genetic analyses of conserved residues in the carboxyl-terminal domain of human immunodeficiency virus type 1 integrase. *J. Virol.* 79, 10356–10368.

Luo, Y., and Muesing, M. A. (2010). Prospective strategies for targeting HIV-1 integrase function. *Future Med. Chem.* 2, 1055–1060.

Maertens, G., Cherepanov, P., Debyser, Z., Engelborghs, Y., and Engelman, A. (2004). Identification and characterization of a functional nuclear localization signal in the HIV-1 integrase interactor LEDGF/p75. *J. Biol. Chem.* 279, 33421–33429.

Maertens, G., Cherepanov, P., Pluymers, W., Busschots, K., De Clercq, E., Debyser, Z., and Engelborghs, Y. (2003). LEDGF/p75 is essential for nuclear and chromosomal targeting of HIV-1 integrase in human cells. *J. Biol. Chem.* 278, 33528–33539.

Masuda, T., Planelles, V., Krogstad, P., and Chen, I. S. (1995). Genetic analysis of human immunodeficiency virus type 1 integrase and the U3 att site: unusual phenotype of mutants in the zinc finger-like domain. *J. Virol.* 69, 6687–6696.

Meister, G., Buhler, D., Pillai, R., Lottspeich, F., and Fischer, U. (2001). A multiprotein complex mediates the ATP-dependent assembly of spliceosomal U snRNPs. *Nat. Cell Biol.* 3, 945–949.

Metifiot, M., Marchand, C., Maddali, K., and Pommier, Y. (2010). Resistance to integrase inhibitors. *Viruses* 2, 1347–1366.

Mohammed, K. D., Topper, M. B., and Muesing, M. A. (2011). Sequential deletion of the integrase (Gag-Pol) carboxyl terminus reveals distinct phenotypic classes of defective HIV-1. *J. Virol.* 85, 4654–4666.

Nakamura, T., Masuda, T., Goto, T., Sano, K., Nakai, M., and Harada, S. (1997). Lack of infectivity of HIV-1 integrase zinc finger-like domain mutant with morphologically normal maturation. *Biochem. Biophys. Res. Commun.* 239, 715–722.

Nishitsuji, H., Hayashi, T., Takahashi, T., Miyano, M., Kannagi, M., and Masuda, T. (2009). Augmentation of reverse transcription by integrase through an interaction with host factor, SIP1/Gemin2 Is critical for HIV-1 infection. *PLoS ONE* 4, e7825. doi:10.1371/journal.pone.0007825

Nomura, Y., Masuda, T., and Kawai, G. (2006). Structural analysis of a mutant of the HIV-1 integrase zinc finger domain that forms a single conformation. *J. Biochem.* 139, 753–759.

Nymark-McMahon, M. H., Beliakova-Bethell, N. S., Darlix, J. L., Le Grice, S. F., and Sandmeyer, S. B. (2002). Ty3 integrase is required for initiation of reverse transcription. *J. Virol.* 76, 2804–2816.

Nymark-McMahon, M. H., and Sandmeyer, S. B. (1999). Mutations in nonconserved domains of Ty3 integrase affect multiple stages of the Ty3 life cycle. *J. Virol.* 73, 453–465.

Shun, M. C., Raghavendra, N. K., Vandegraaff, N., Daigle, J. E., Hughes, S., Kellam, P., Cherepanov, P., and Engelman, A. (2007). LEDGF/p75 functions downstream from preintegration complex formation to effect gene-specific HIV-1 integration. *Genes Dev.* 21, 1767–1778.

Summa, V., Petrocchi, A., Bonelli, F., Crescenzi, B., Donghi, M., Ferrara, M., Fiore, F., Gardelli, C., Gonzalez Paz, O., Hazuda, D. J., Jones, P., Kinzel, O., Laufer, R., Monteagudo, E., Muraglia, E., Nizi, E., Orvieto, F., Pace, P., Pescatore, G., Scarpelli, R., Stillmock, K., Witmer, M. V., and Rowley, M. (2008). Discovery of raltegravir, a potent, selective orally bioavailable HIV-integrase inhibitor for the treatment of HIV-AIDS infection. *J. Med. Chem.* 51, 5843–5855.

Tsurutani, N., Kubo, M., Maeda, Y., Ohashi, T., Yamamoto, N., Kannagi, M., and Masuda, T. (2000). Identification of critical amino acid residues in human immunodeficiency virus type 1 IN required for efficient proviral DNA formation at steps prior to integration in dividing and nondividing cells. *J. Virol.* 74, 4795–4806.

Wang, J. Y., Ling, H., Yang, W., and Craigie, R. (2001). Structure of a two-domain fragment of HIV-1 integrase: implications for domain organization in the intact protein. *EMBO J.* 20, 7333–7343.

Wilkinson, T. A., Januszyk, K., Phillips, M. L., Tekeste, S. S., Zhang, M., Miller, J. T., Le Grice, S. F., Clubb, R. T., and Chow, S. A. (2009). Identifying and characterizing a functional HIV-1 reverse transcriptase-binding site on integrase. *J. Biol. Chem.* 284, 7931–7939.

Wu, X., Liu, H., Xiao, H., Conway, J. A., Hehl, E., Kalpana, G. V., Prasad, V., and Kappes, J. C. (1999). Human immunodeficiency virus type 1 integrase protein promotes reverse transcription through specific interactions with the nucleoprotein reverse transcription complex. *J. Virol.* 73, 2126–2135.

Zhu, K., Dobard, C., and Chow, S. A. (2004). Requirement for integrase during reverse transcription of human immunodeficiency virus type 1 and the effect of cysteine mutations of integrase on its interactions with reverse transcriptase. *J. Virol.* 78, 5045–5055.

Conflict of Interest Statement: The author declares that the research was conducted in the absence of any commercial or financial relationships that could be construed as a potential conflict of interest.

Received: 14 September 2011; paper pending published: 24 September 2011; accepted: 26 September 2011; published online: 13 October 2011.

Citation: Masuda T (2011) Non-enzymatic functions of retroviral integrase: the next target for novel anti-HIV drug development. Front. Microbio. 2:210. doi: 10.3389/fmicb.2011.00210

This article was submitted to Frontiers in Virology, a specialty of Frontiers in Microbiology.

OPEN ACCESS Freely available online

PLoS one

Nuclear Exportin Receptor CAS Regulates the NPI-1–Mediated Nuclear Import of HIV-1 Vpr

Eri Takeda[1], Tomoyuki Murakami[1,2], Go Matsuda[1], Hironobu Murakami[1,3], Tamotsu Zako[4], Mizuo Maeda[4], Yoko Aida[1,2]*

1 Viral Infectious Diseases Unit, RIKEN, Hirosawa, Wako, Saitama, Japan, **2** Laboratory of Viral Infectious Diseases, Department of Medical Genome Sciences, Graduate School of Frontier Science, The University of Tokyo, Wako, Saitama, Japan, **3** Japan Foundation for AIDS Prevention, Chiyoda-ku, Tokyo, Japan, **4** Bioengineering Laboratory, RIKEN, Hirosawa, Wako, Saitama, Japan

Abstract

Vpr, an accessory protein of human immunodeficiency virus type 1, is a multifunctional protein that plays an important role in viral replication. We have previously shown that the region between residues 17 and 74 of Vpr (Vpr_{N17C74}) contained a bona fide nuclear localization signal and it is targeted Vpr_{N17C74} to the nuclear envelope and then imported into the nucleus by importin α (Impα) alone. The interaction between Impα and Vpr is important not only for the nuclear import of Vpr but also for HIV-1 replication in macrophages; however, it was unclear whether full-length Vpr enters the nucleus in a manner similar to Vpr_{N17C74}. This study investigated the nuclear import of full-length Vpr using the three typical Impα isoforms, Rch1, Qip1 and NPI-1, and revealed that full-length Vpr is selectively imported by NPI-1, but not Rch1 and Qip1, after it makes contact with the perinuclear region in digitonin-permeabilized cells. A binding assay using the three Impα isoforms showed that Vpr bound preferentially to the ninth armadillo repeat (ARM) region (which is also essential for the binding of CAS, the export receptor for Impα) in all three isoforms. Comparison of biochemical binding affinities between Vpr and the Impα isoforms using surface plasmon resonance analysis demonstrated almost identical values for the binding of Vpr to the full-length isoforms and to their C-terminal domains. By contrast, the data showed that, in the presence of CAS, Vpr was released from the Vpr/NPI-1 complex but was not released from Rch1 or Qip1. Finally, the NPI-1–mediated nuclear import of Vpr was greatly reduced in semi-intact CAS knocked-down cells and was recovered by the addition of exogenous CAS. This report is the first to show the requirement for and the regulation of CAS in the functioning of the Vpr-Impα complex.

Citation: Takeda E, Murakami T, Matsuda G, Murakami H, Zako T, et al. (2011) Nuclear Exportin Receptor CAS Regulates the NPI-1–Mediated Nuclear Import of HIV-1 Vpr. PLoS ONE 6(11): e27815. doi:10.1371/journal.pone.0027815

Editor: Roberto F. Speck, University Hospital Zurich, Switzerland

Received January 27, 2011; **Accepted** October 26, 2011; **Published** November 16, 2011

Funding: This work was supported by a Health Sciences Research Grant from the Ministry of Health, Labor and Welfare of Japan (Research on HIV/AIDS: http://www.jhsf.or.jp/English/index_e.html) and by the program for Promotion of Fundamental Studies in Health Sciences of the National Institute of Biomedical Innovation (NIBIO) of Japan (ID 06-01: http://www.nibio.go.jp/english/index.html). The funders had no role in study design, data collection and analysis, decision to publish, or preparation of the manuscript. No additional external funding received for this study.

Competing Interests: The authors have declared that no competing interests exist.

* E-mail: aida@riken.jp

Introduction

Molecular trafficking between the nucleus and the cytoplasm is tightly regulated in eukaryotic cells. Nuclear import processes involve the nuclear pore complexes (NPCs) of the nuclear envelope and, typically, require nuclear localization signals (NLSs). The nuclear import of classical NLS-bearing proteins is mediated by specific soluble factors, including Importin (Imp), which consists of two subunits, Impα and Impβ, small GTPase Ran/TC4, and nuclear transport factor 2 [1]. The ternary complex with NLS-bearing protein, Impα, and Impβ translocates into the nucleus, and the binding GTP-bound form of Ran to Impβ triggers the dissociation of ternary complex, releasing Impα [2]. However, there are many additional pathways that mediate nuclear import; for example, Impβ-like molecules (such as the transport factor for substrates carrying the M9 shuttling signal or importin 7) and Impβ itself are competent to transfer some cargo by themselves [3]. In addition, it was previously reported that Impα could migrate into the nucleus in an Impβ- and Ran-independent manner [4]. Impα alone can escort Vpr, one of the accessory proteins of human immunodeficiency virus type 1 (HIV-1) [5,6], as well as Ca^{2+}/calmodulin-dependent protein kinase type IV (CaMKIV) into the nucleus without utilizing the classical Impβ-dependent transport system [7].

Impα is composed of a flexible N-terminal Impβ-binding (IBB) domain and a highly structured domain comprising ten tandem armadillo (ARM) repeats [2]. The helical ARM repeats assemble into a twisted slug-like structure whose belly serves as the NLS-binding groove. The central portion of Impα, which contains the ARM repeats, recognizes the NLS cargo, while its N-terminal basic region, termed the IBB domain, binds to Impβ, and the region between residues 383 and 497, corresponding to the ninth and tenth ARM regions, binds to the cellular apoptosis susceptibility (CAS) protein [2,8]. The crystal structure of Impα has shown that the region between residues 469 and 478, within the tenth ARM region, contains the core sequences for CAS binding [8]. The nature of the dissociation of the NLS cargo from Impα is unclear, but it has been proposed that nucleoporins (Nups), together with CAS, assist in the dissociation process [2,9]. CAS binds preferentially to Impα, after its

dissociation from the NLS cargo, and exports nuclear Impα to the cytoplasm. However, Impα has at least seven isoforms in human [2,10,11], grouped into three subfamilies (α1, α2 and α3) based on their amino acid sequence similarities. There is approximately 80–90% sequence homology in each subfamily [2,12]. Subfamily α1 includes importin α5 (NPI-1/SPR1/karyopherin alpha 1 [KPNA1]), importin α6 (KPNA5) and importin α7 (KPNA6). Subfamily α2 contains importin α1 (Rch1/SRP1α/KPNA2) and the recently-reported importin α8 (KPNA7) [10,11]. Subfamily α3 includes importin α3 (Qip1/SRP3/KPNA4) and importin α4 (KPNA3). Members of the three subfamilies have about 50% homology with each other [2,12]. Many studies have shown that Impα isoforms differ in their efficiencies with respect to classical substrate-specific import, show unique expression patterns in various tissues and cells, and depend on the state of cellular metabolism and differentiation [2,6,13]. Taken together, this information suggests that Impα proteins contribute primarily to tissue-specific nuclear transport.

Vpr has multiple biological functions, including nuclear localization activity [14,15,16], arresting cells at the G2/M phase of the cell cycle [17,18,19], increasing the activity of the HIV-1 long terminal repeat [20], selective inhibition of cellular pre-mRNA splicing both *in vivo* and *in vitro* [21,22], and positive and negative regulation of apoptosis [23]. These functions are carried out through interactions with a variety of cellular partners. Especially, the virion-associated viral protein, Vpr, is necessary for the nuclear import of the viral pre-integration complex (PIC) in non-dividing cells [6,14,15,24], although its exact role in the PIC entry mechanism remains unclear. There are several pathways that Vpr could use to cross the nuclear envelope. First, numerous investigations regarding the subcellular localization of Vpr suggest that the Vpr protein may cross the nuclear envelope by passive diffusion, as it is small enough (15 kDa) to pass through the NPC [15,25]. Second, Vpr enters the nucleus by interacting with nucleoporins, which are constituents of the NPC [26,27,28]. Third, Vpr binds to Impα , which stimulates subsequent nuclear import of the cargo by increasing the affinity of Impα for NLS-containing proteins [16]. Another report describes a novel nuclear import mechanism for Vpr, involving two putative alpha-helical domains, located between residues 17 and 34 (αH1) and between residues 46 and 74 (αH3), which are required for the nuclear localization of Vpr [25]. A subsequent study used microinjection and *in vitro* transport assays incorporating the chimeric protein Vpr_{N17C74} to show that the entire region between residues 17 and 74 is a bona fide NLS [5]. Furthermore, an *in vitro* transport assay experiment designed to identify the factors required for Vpr_{N17C74} nuclear entry found that Vpr itself is targeted to the nuclear envelope and is then transported by Impα, without any involvement of Impβ [5]. The three typical Impα isoforms, Rch1, Qip1 and NPI-1, appear able to interact directly with Vpr_{N17C74} and support its nuclear entry. Interestingly, the interaction between Impα and Vpr is necessary not only for the nuclear import of Vpr but also for HIV-1 replication in macrophages [6]. These results suggest that the interaction between Vpr and Impα may be a potential target for therapeutic intervention. Indeed, a potential parent compound, hematoxylin, has been identified, which suppresses the Vpr_{N17C74}-Impα interaction, thereby inhibiting the nuclear import of the HIV-1 viral genome in macrophages in a Vpr-dependent manner [29].

A nuclear magnetic resonance structural analysis revealed that full-length Vpr forms three amphipathic alpha helices surrounding a hydrophobic core [30,31]. It has a flexible, negatively-charged N-terminal domain flanking the helices and its C-terminal domain is also flexible, positively charged, and rich in arginine residues [30,31]. Two motifs, amino acids 56 to 77 in the third α-helical domain (αH3) and amino acids 77 to 96 in the arginine-rich C-terminal domain, are critical for the inhibition of pre-mRNA splicing by Vpr [20], while the C-terminal domain appears to be critical for Vpr-induced G2 arrest and apoptosis [32,33]. The N-terminal domain was shown to be important for localization to the nuclear rim [34]. Taken together, these results clearly indicate that the N-terminal and the C-terminal Vpr domains play critical roles in the multiple functions of Vpr. However, it is unclear whether full-length Vpr enters the nucleus in a manner similar to that of the chimeric protein, Vpr_{N17C74}. In this investigation, we have studied the detailed mechanism of full-length Vpr entry into the nucleus. Using a digitonin-permeabilized transport assay, the nuclear import of full-length Vpr by the three major isoforms of Impα, Rch1, Qip1 and NPI-1, was analyzed. Furthermore, to clarify the means by which NPI-1 selectively transports full-length Vpr, the Impα isoform domain involved in the interaction with Vpr and these accurate binding affinities were identified using a glutathione-S-transferase (GST)-pull down assay and surface plasmon resonance (SPR). Moreover, we used a GST pull-down assay to show that although Vpr binds to the CAS-binding domain of all of three Impα isoforms to roughly the same extent, CAS can dissociate the interaction between Vpr and NPI-1 but not between Vpr and Rch1 or Qip1. Finally, we used an *in vitro* nuclear import assay using HeLa cells with knocked-down CAS to demonstrate that CAS is required for the nuclear entry of full-length Vpr.

Results

Full-length Vpr is preferentially imported into nuclei by Impα5 (NPI-1)

A chimeric protein comprising full-length Vpr fused at the N-terminus to GST and green fluorescent protein (GFP) (~63 kDa) was constructed, which surpassed the limit for passive diffusion into the nucleus (**Fig. 1A**). An *in vitro* nuclear import assay was then performed using digitonin-permeabilized, semi-intact HeLa cells (**Fig. 1B**). In the absence of soluble factors, full-length Vpr localized predominantly to the perinuclear region in a manner similar to that of the Vpr_{N17C74} mutant. By contrast, no signal was detected in the perinuclear region when using a negative control protein (a chimeric GST-GFP protein). Interestingly, the nuclear import of Vpr changed significantly in the presence of the different Impα isoforms. High levels of Vpr entered the nucleus in the presence of NPI-1; however, the levels were much lower in the presence of Qip1, and no entry was observed in the presence of Rch1. By contrast, in agreement with a previous report [6], the Vpr_{N17C74} mutant entered the nucleus at similar levels in the presence of all three Impα isoforms. GST-GFP failed to enter the nucleus, even in the presence of all three Impα isoforms.

Next, the extent of the nuclear import activity exhibited by Vpr in the presence of 0.25, 0.5, 1 or 2 μM of the Impα isoforms was examined by measuring the fluorescence intensity in the nucleus (**Fig. 1C**). Only NPI-1 efficiently enhanced the nuclear import of Vpr. Qip1 showed a very weak effect on the nuclear entry of Vpr, which remained at a low level even in the presence of 2 μM Qip1. By contrast, no nuclear import of Vpr was detected in the presence of Rch1, even at a concentration of 2 μM.

The effect of Rch1 and Qip1 on the nuclear entry of full-length Vpr mediated by NPI-1 was then examined (**Fig. 1D**). NPI-1–mediated nuclear import of Vpr did not decrease in the presence of Rch1 or Qip1. Moreover, the Impα isoform-driven nuclear import of Vpr was completely inhibited when Impβ was added to semi-intact HeLa cells (**Fig. 1E**). Likewise, Impβ decreased the nuclear import of the Vpr_{N17C74} mutant in the presence of Rch1 (**Fig. 1E**). Taken together, these results suggest that full-length Vpr is targeted to the perinuclear region and is then transported into the nucleus by NPI-1 alone, without any requirement for Impβ.

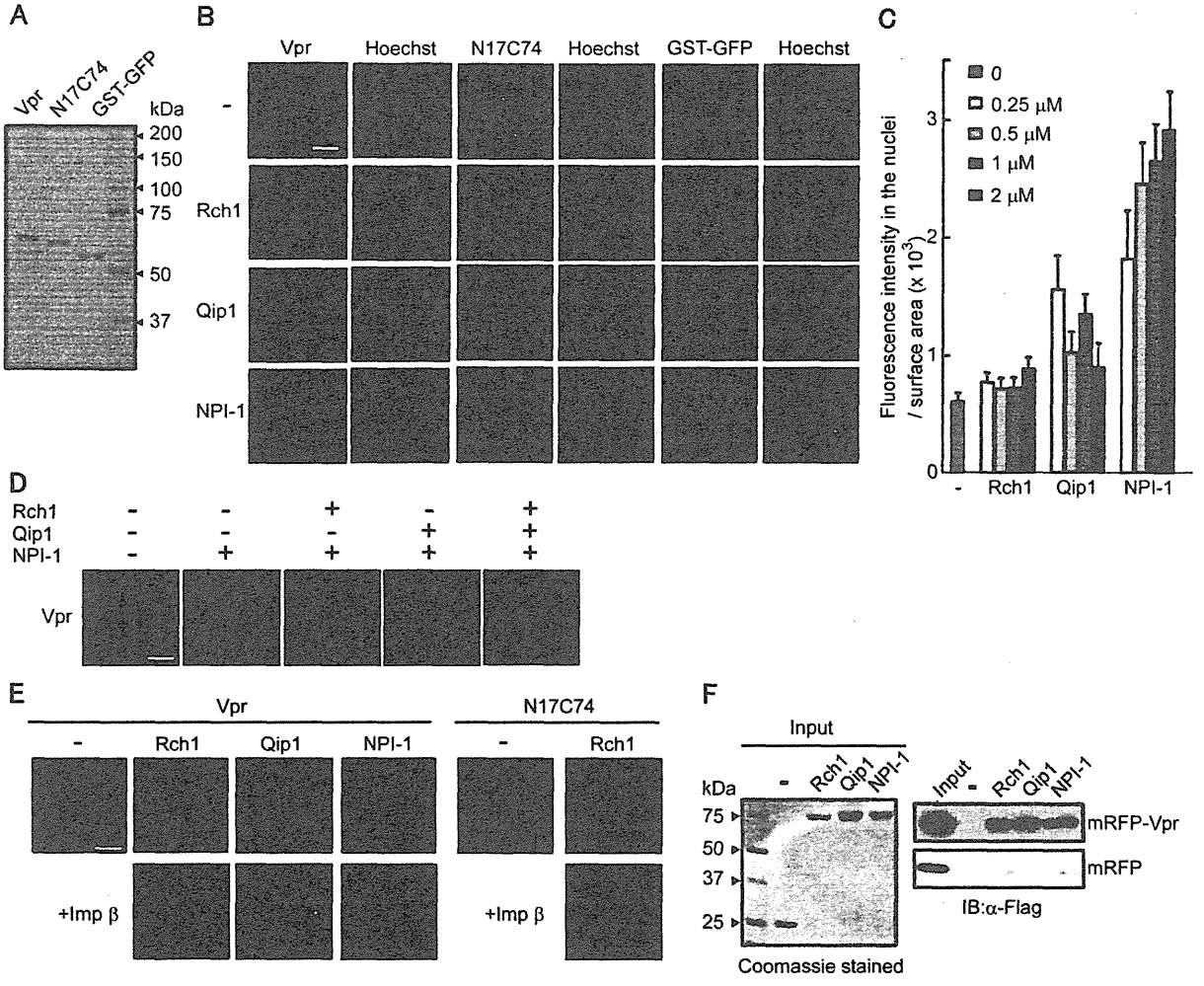

Figure 1. Importin α5/NPI-1 preferentially mediates the nuclear import of Vpr. (A) Twenty-five pmol of purified recombinant GST- and GFP-tagged Vpr (Vpr), GST- and GFP- tagged Vpr_{N17C74} (N17C74), GST-tagged GFP (GST-GFP) were resolved by 10% SDS-PAGE and stained with Coomassie brilliant blue (CBB). (B) Nuclear import of Vpr by importin α (Impα) isoforms. Digitonin-permeabilized HeLa cells were incubated with 1 μM of Vpr, N17C74, and GST-GFP in the absence (-) or presence of 1 μM (for Vpr and GST-GFP) or 3 μM (for N17C74) of each of the recombinant Impα isoforms, Rch1, Qip1 and NPI-1. Cells were fixed in 3.7% formaldehyde and stained with Hoechst 33342 to show the position of the nucleus (right panel). After fixation, cells were analyzed by confocal laser scanning microscopy. Bar = 10 μm. (C) Fluorescence intensity of Vpr per surface area was quantified for at least 70 nuclei in the presence of the indicated concentrations of the Impα isoforms from three independent experiments. The bar shows the standard errors of measurements. (D) *In vitro* nuclear import assay for GST-GFP-Vpr was performed in the absence (-) or presence of 1 μM of the Impα isoforms. After fixation, cells were analyzed by confocal microscopy. Bar = 10 μm. (E) *In vitro* nuclear import assay for Vpr was performed in the absence (-) or presence of 1 μM of the Impα isoforms, and 1 μM of Impα isoforms with 1 μM Impβ. N17C74, as a control, was performed with 1 μM of Rch1 and 1 μM Impβ. After fixation, cells were analyzed by confocal microscopy. Bar = 10 μm. (F) Binding assay between Vpr and the Impα isoforms. Glutathione-Sepharose beads were coupled with the GST-Impα isoforms, Rch1, Qip1 and NPI-1 or GST alone, and were incubated with Vpr protein purified from 293T cells transfected with pCAGGS mammalian vectors encoding Flag-mRFP (mRFP), or Flag-mRFP-Flag-Vpr (mRFP-Vpr). The bound fractions and 1/20 of the input of mRFP-Vpr and mRFP were analyzed by immunoblotting with an anti-Flag M2 monoclonal antibody (MAb) (right panel). Twenty-five pmol of GST or GST-Impα isoforms were resolved by 10% SDS-PAGE and stained with CBB (left panel). The positions of mRFP and mRFP-Vpr are indicated.

doi:10.1371/journal.pone.0027815.g001

Full-length Vpr interacts with all three Impα isoforms

To examine further whether full-length Vpr interacts directly with all three Impα isoforms, the recombinant GST-tagged Impα isoforms, Rch1, Qip1 and NPI-1 (immobilized on glutathione-Sepharose beads), were incubated with mRFP-Vpr purified from vertebrate cells. Interestingly, full-length Vpr was able to interact with all three isoforms (**Fig. 1F**), indicating that Vpr is able to bind directly to Rch1 and Qip1, even though these isoforms did not promote its nuclear entry as well as did NPI-1, which showed preferential transport of Vpr into the nucleus.

Full-length Vpr binds to the Impα CAS-binding domain

Since the three major Impα isoforms, Rch1, Qip1 and NPI-1, share approximately 50% overall amino acid sequence similarity [2,12], we decided to determine whether the same domain was involved in binding full-length Vpr in all three isoforms. Impα is

composed of an N-terminal IBB domain, a highly-structured domain comprised of ten tandem ARM repeats and a C-terminal acidic domain [2], as shown in **Fig. 2A**. For each isoform, three truncated mutants were prepared as fusion proteins with GST: 1) the IBB domain mutant, 2) the mutant containing the ARM repeat domain but lacking the tenth ARM repeat, and 3) the mutant including the C-terminal region between the ninth ARM repeat and the acidic domain, (**Fig. 2B**). These mutants were then assessed for their binding activity with full-length Vpr (**Fig. 2D**). The recombinant mutant corresponding to the ARM repeat domain between residues 70 to 438 of Rch1 was very unstable and was difficult to purify; therefore, a slightly extended form of the mutant, between residues 70 to 475 but without the tenth ARM repeat, was used.

Vpr bound to all mutants of all three Impα isoforms: two of the deletion mutants, the ARM repeat domain lacking the tenth ARM repeat ($Rch1_{70-475}$, $Qip1_{69-439}$ and $NPI\text{-}1_{76-451}$) and the C-terminal region containing the ninth ARM repeat ($Rch1_{404-529}$, $Qip1_{392-537}$ and $NPI\text{-}1_{76-541}$), bound to Vpr with the same level as full-length Impα. The IBB domain mutant ($Rch1_{1-69}$, $Qip1_{1-68}$ and $NPI\text{-}1_{1-75}$) also interacted with Vpr, albeit with lower affinities than those shown by the full-length Impα isoforms. These results suggested that the main Vpr binding site is located somewhere between the structural ARM repeats and the C-terminal region but is not found in the IBB domain for all three Impα isoforms.

The two mutant forms that bound strongly to Vpr, as mentioned above, shared the ninth ARM repeat (**Fig. 2A**). Therefore, different truncated forms lacking the ninth ARM repeat ($Rch1_{70-403}$, $Qip1_{69-391}$ and $NPI\text{-}1_{76-403}$) were constructed (**Fig. 2C**) and a pull-down assay was performed using mRFP-Vpr (**Fig. 2E**). The binding of the ARM repeat mutants lacking the ninth ARM repeat to Vpr was reduced significantly, indicating that the ninth ARM repeat region of all of three Impα isoforms ($Rch1_{404-475}$, $Qip1_{392-439}$ and $NPI\text{-}1_{404-451}$) is the major binding site for full-length Vpr.

Full-length Vpr binds with similar affinity to the C-terminal domain of the three Impα isoforms

To quantify the binding affinities between Vpr and each of the Impα isoforms accurately, the BIAcore 2000 SPR sensor system was used. In this system, four samples can be immobilized individually on the same chip, and their interactions with analytes can be tested simultaneously. Each of the three recombinant full-length Impα isoforms and their C-terminal peptide mutants ($Rch1_{404-529}$, $Qip1_{392-537}$ and $NPI\text{-}1_{76-541}$), the GST was cleaved with PreScission protease, were immobilized on one lane of a sensor chip and a remaining vacant lane was used as a negative control for the non-specific binding of GST-Vpr and GST to the chip. The chip-bound Impα isoforms were exposed to various concentrations of GST-Vpr and GST, and their affinity constants were measured by analyzing the curves (**Fig. 3**). Typical sensor curves of various Vpr concentrations (0 to 40 μM) interacting with full-length NPI-1 ($NPI\text{-}1_{full}$) are shown in **Fig. 3A**. The binding affinities obtained are summarized in **Table 1**. The K_D values for the full-length Vpr-Impα isoform interactions were very similar: 8.9 μM (Rch1), 6.8 μM (Qip1), and 7.4 μM (NPI-1). The K_D values for two of the Vpr-Impα C-terminal peptides were similar to those for the full-length Impα isoforms, 6.5 μM ($Qip1_{392-537}$) and 6.7 μM ($NPI\text{-}1_{404-541}$); however, the K_D of the Rch1 C-terminal peptide, 4.3 μM ($Rch1_{404-529}$), showed a two-fold decrease compared with the K_D of full-length Rch1. This experiment confirmed that the binding affinities between Vpr and all Impα isoforms are very similar.

CAS disrupts the interaction between Vpr and NPI-1, but not between Vpr an Rch1 or Qip1

The sequences required for binding to the CAS nuclear export factor are located between the ninth and tenth ARM repeats within Impα [2]. The present study indicated that the ninth ARM repeat of Impα is the main region involved in binding to Vpr and is also necessary for the interaction with CAS. Therefore, to determine whether CAS affects the interaction between Vpr and Impα, glutathione-sepharose beads coupled to GST-Rch1, -Qip1 or -NPI-1 were incubated with mRFP-Vpr in the absence or presence of purified recombinant CAS and a RanGTP analog (Q69LRanGTP) (**Fig. 4A**). RanGTP is necessary for the interaction between Impα and CAS in cell nuclei. As shown in **Fig. 4B and C**, the amount of Vpr bound to NPI-1 decreased as the concentration of CAS increased in the presence of Q69LRanGTP in a dose-dependent manner (a 0.2-fold difference in the presence of 50 pmoles CAS). This was not the case for Rch1 and Qip1, indicating that CAS causes the dissociation of Vpr from NPI-1 (which can import the full-length Vpr into the nucleus) but does not disrupt Vpr/Rch1 or Vpr/Qip1 interactions, which are not involved in Vpr nuclear import. When Q69LRanGTP was absence on Pull-down assay, CAS only showed a very weak effect on the dissociation of Vpr from NPI-1 (**Fig. 4D**).

CAS regulates the NPI-1–mediated nuclear entry of full-length Vpr

Finally, the requirement for CAS for NPI-1–mediated nuclear entry of full-length Vpr was confirmed using an *in vitro* nuclear import assay. The results clearly showed that the expression of the endogenous CAS protein was not affected by digitonin-induced permeabilization (**Fig. S1**). Therefore, an *in vitro* nuclear import assay was performed using HeLa cells in which CAS expression had been knocked down. Knock-down was confirmed by immunoblotting experiments conducted after a 36 h treatment with two siRNAs (siRNA1 and siRNA2) against CAS mRNA (**Fig. 5A**). HeLa cells were permeabilized with digitonin and used in an *in vitro* import assay (**Fig. 5B, C**). The nuclear import of GST-GFP-Vpr, which was enhanced by the addition of NPI-1, was greatly decreased in HeLa cells treated with either CAS-specific siRNA1 or siRNA2, but not in negative control siRNA-transfected cells or in untreated cells. Furthermore, this reduction in nuclear import was rescued by up to 50% by the addition of exogenous CAS (recovery was considered to be 50% because exogenous CAS needs time to reach the cell nuclei). However, Vpr was able to localize to the nuclear envelope in these cells, indicating that CAS has no effect on the perinuclear localization of Vpr, an event that does not require both Impα isoforms. These results clearly demonstrate that CAS is essential for the NPI-1–mediated nuclear import of Vpr.

Discussion

This study investigated the nuclear import of full-length Vpr, the HIV-1 accessory protein, using an *in vitro* nuclear import assay with digitonin-permeabilized HeLa cells and a pull-down assay. The results produced two major conclusions: first, the data suggested that full-length Vpr is preferentially imported into the nucleus by NPI-1 but not Rch1 and Qip1, in contrast with Vpr_{N17C74}, which can be imported by all three major isoforms of Impα [6]. Certain previous studies have shown that each Impα isoform imports different viral proteins; for example, Qip1 interacts with HIV-1 integrase (IN) and contributes to HIV-1 nuclear import and replication [35], while NPI-1 and Rch1 interact with the influenza virus Nucleoprotein to promote its

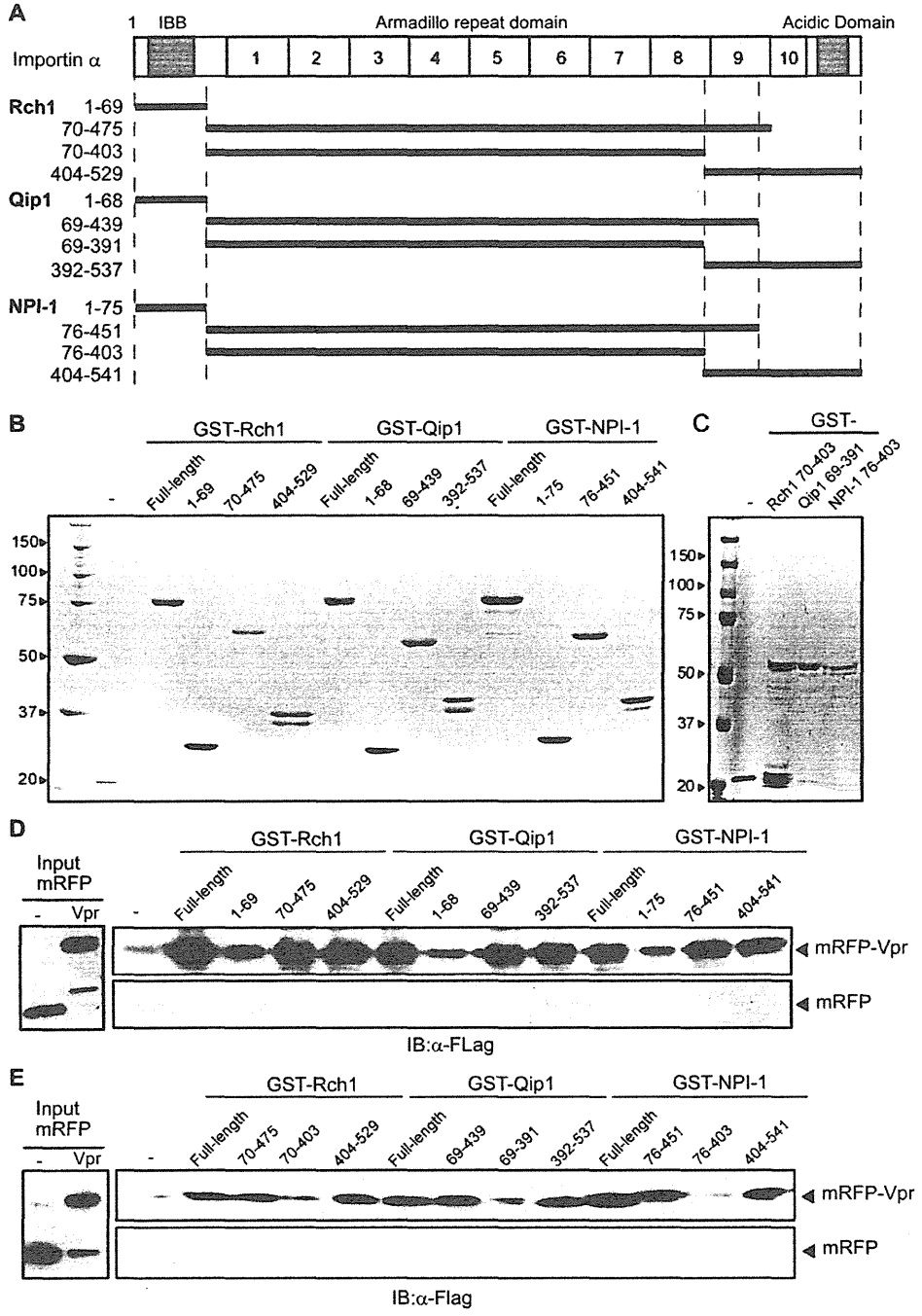

Figure 2. Mapping of the Impα isoform domains involved in the interaction with Vpr. (A) Schematic representation of the Impα isoforms, Rch1, Qip1, NPI-1 and their deletion mutants. (B and C) All mutants were expressed as GST fusion proteins in *E. coli* and purified using Glutathione-Sepharose. Twelve pmol of purified GST-tagged Impα isoform derivatives were resolved by 10% SDS-PAGE and stained with CBB. (D and E) Binding of Impα isoforms to Vpr. Glutathione-Sepharose beads coupled to GST-Impα isoforms or GST alone were incubated with mRFP-Vpr or mRFP. The bound fractions and 1/50 of the input of mRFP-Vpr and mRFP were analyzed by immunoblotting with anti-Flag M2 MAb (right panel). The positions of mRFP and mRFP-Vpr are indicated.
doi:10.1371/journal.pone.0027815.g002

nuclear import [36]. Second, our data from the *in vitro* nuclear import assay using HeLa cells with the knocked-down nuclear export receptor, CAS, indicated that CAS is essential for the NPI-1–mediated nuclear import of Vpr. We also showed that CAS mediated the release of Vpr from NPI-1 but not from Rch1 and Qip1, thus facilitating the transport of Vpr into the nucleus. It was

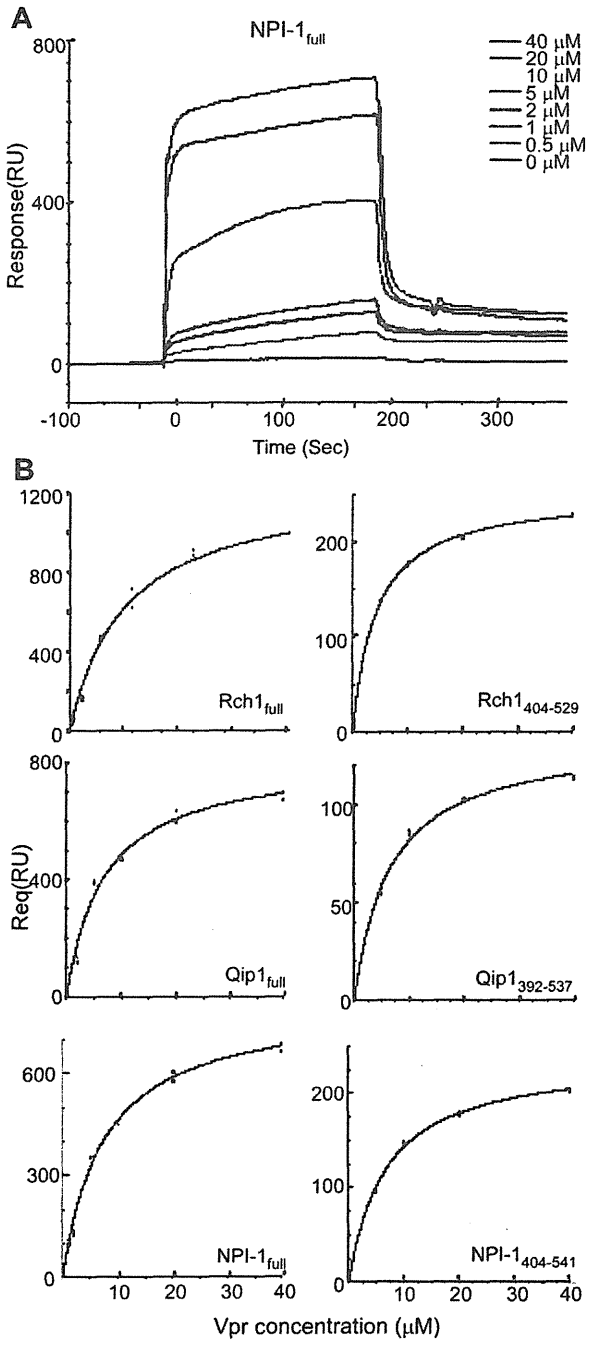

Figure 3. SPR measurements of the interaction between Vpr and full-length or C-terminal Impα isoforms using BIAcore. (A) SPR sensorgrams of the interactions between GST-Vpr and the full-length Impα isoform, NPI-1_{full}, immobilized to the CM sensor chip. Sensor curves of the interactions between Vpr at various concentrations (0 to 40 μM) and NPI-1_{full} are shown. (B) The analysis curves used to obtain the dissociation constants (K_D) for the interactions between Vpr and the Impα isoforms, Rch1_{full}, Qip1_{full}, NPI-1_{full}, Rch$1_{404-529}$, Qip$1_{392-537}$ and NPI$1_{404-541}$ using the steady state binding model equation (see Material and Methods).
doi:10.1371/journal.pone.0027815.g003

Table 1. Dissociation equilibrium constants determined using BIAcore.

Analite	Ligand	KD (M)	Ligand	KD (M)
Vpr	Rch1_{full}	8.9×10^{-6}	Rch$1_{404-529}$	4.3×10^{-6}
	Qip1_{full}	6.8×10^{-6}	Qip$1_{392-537}$	6.5×10^{-6}
	NPI-1_{full}	7.4×10^{-6}	NPI-$1_{404-541}$	6.7×10^{-6}

Dissociation equilibrium constants determined using BIAcore. K_D of Vpr was determined by using the Vpr sensorgrams obtained by subtracting GST sensorgrams from GST-Vpr sensorgrams at the same concentrations. *Full*: full-length.
doi:10.1371/journal.pone.0027815.t001

known, from previous reports, that in the classical nuclear import of the NLS cargo/Impα/Impβ complex, CAS increased the dissociation of the Impα/NLS cargo complex together with nucleoporins, such as Nup50, after the dissociation of Impβ from the ternary complex in the nucleus [2,37,38]. However, a requirement for CAS in this process had not previously been confirmed by *in vitro* nuclear import assay. In addition, it was previously reported that although CaMKIV, which is transported by Impα without utilizing Impβ, binds to the C-terminal region of mouse Rch1 (Rch$1_{413-459}$) in a similar manner to Vpr, the interaction between Impα and CaMKIV was not disrupted by the addition of CAS in a solution-binding assay [7]. Therefore, this study is the first to demonstrate, using *in vitro* nuclear import and pull-down assays, that CAS is required for Impα-mediated nuclear import and plays a direct role in the regulation of the NLS cargo-Impα complex without utilizing the Impβ-dependent transport pathway.

Our present and previous results have allowed us to characterize the mechanism governing the entry of full-length Vpr into the nucleus as follows: i) full-length Vpr localizes to the perinuclear region, without a requirement for soluble factors, before it is transported into the nucleus by Impα, as shown by the *in vitro* nuclear import assays using digitonin-permeabilized HeLa cells (**Fig. 1**) and CAS-specific siRNA-treated permeabilized HeLa cells (**Fig. 5**). This perinuclear localization in the absence of Impα isoforms is in agreement with the nuclear import of Vpr_{N17C74} (**Fig. 1B**) [6] and distinguishes the nuclear import of Vpr from that of other NLS-bearing proteins. ii) The detailed binding assay with truncated forms of the three Impα isoforms showed that full-length Vpr binds preferentially to the ninth ARM repeat, which is also the domain required for CAS interaction with Impα. This data partially agrees with a previous report in which Vpr_{N17C74} required the C-terminal peptide of Impα directly to entry into nucleus, though it majorly bound to IBB domain of the Impα [5]. iii) Our SPR analysis clearly demonstrated similar binding affinities for Vpr to each of the three full-length Impα isoforms as well as to their C-terminal domains, which contained the ninth ARM region, identified as the major Vpr-binding site, and also the CAS binding site [8,37]. iv) This study demonstrated that the release of Vpr from the Vpr/NPI-1 complex depends on CAS. By contrast, CAS did not cause the dissociation of Vpr from complexes with Rch1 or Qip1, even though they were capable of importing Vpr into the nucleus (**Fig. 4B, C**). v) We also showed that the nuclear import of Vpr by NPI-1 was not affected by Rch1 or Qip1 (**Fig. 1D**), suggesting that each of the Impα isoforms exist in equilibrium with Vpr in the cytoplasm. It was assumed that all the Impα isoforms have same binding affinity for Vpr (**Fig. 3** and **Table 1**). vi) After interacting with Impα at the perinuclear region, full-length Vpr was selectively imported by NPI-1 but not